Computed Tomography 2.0

Photon-Counting and Artificial Intelligence

Marc Kachelrieß

German Cancer Research Center (DKFZ)
Heidelberg, Germany
www.dkfz.de/ct

PHOTON-COUNTING CT

Availability of Diagnostic Photon-Counting CT

	Sensor material	Detector pixel size at iso	Pixel binning	FOM	Bins	FDA	Pubs	Installations
Canon	CdZnTe	210 µm	3×3, 1×1	50 cm	5	no	1	1 prototype (Japan)
GE	Si, edge on	400 × 400 µm	?	?	?	no		1 experimental (Sweden), 2 prototypes (USA)
Philips	CdZnTe	274 × 274 µm	?	50 cm	5	no	≈22	1 experimental setup (France)
Samsung Omnitom Elite	CdTe	703 × 707 µm / 351 × 423 µm / 117 × 141 µm	5×6, 3×3, 1×1	30 cm	3	yes	1	?
Siemens CounT	GOS/CdTe dual source	700 × 600 µm / 250 × 250 µm	2×2, 1×1	50 / 28 cm	4	no	≈50	3 experimental systems (Germany, USA)
Siemens CountPlus	CdTe	150 × 176 µm	2×2, 1×1	50 cm	4	no	≈11	3 prototypes (Czech, Sweden, USA)
Siemens Alpha	CdTe/CdTe dual source	2 · 150 × 176 µm	2×2, 1×1	50 / 36 cm	4	yes	≈40	about 100 worldwide

Edge on design (Si only)

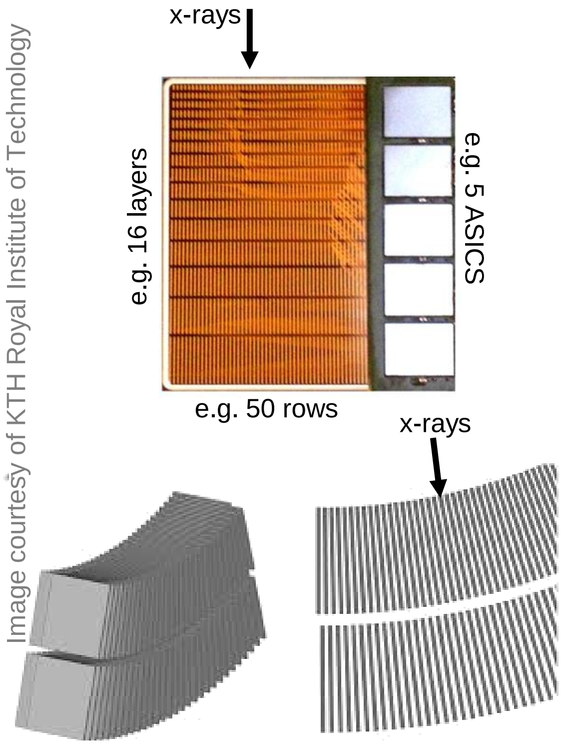

Face on design (all others)

Image courtesy of Siemens Healthineers

The additional factor 2 in the detector pixel size column indicates that some scan modes may use binning.

dkfz.

Diagnostic CT (Conventional Detector) of a Low Contrast Phantom

Photon Counting Detector CT of a Low Contrast Phantom

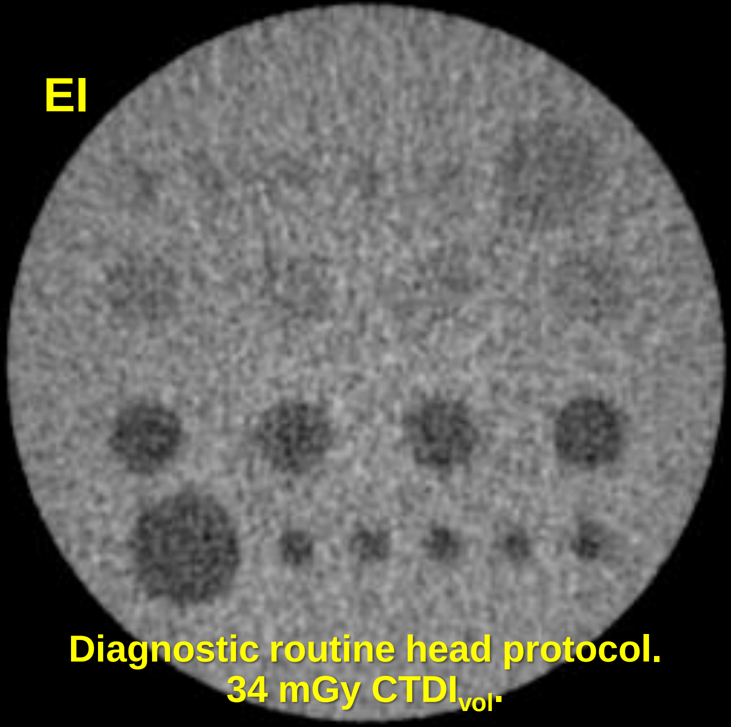

Diagnostic routine head protocol.
34 mGy $\mathrm{CTDI_{vol}}$.

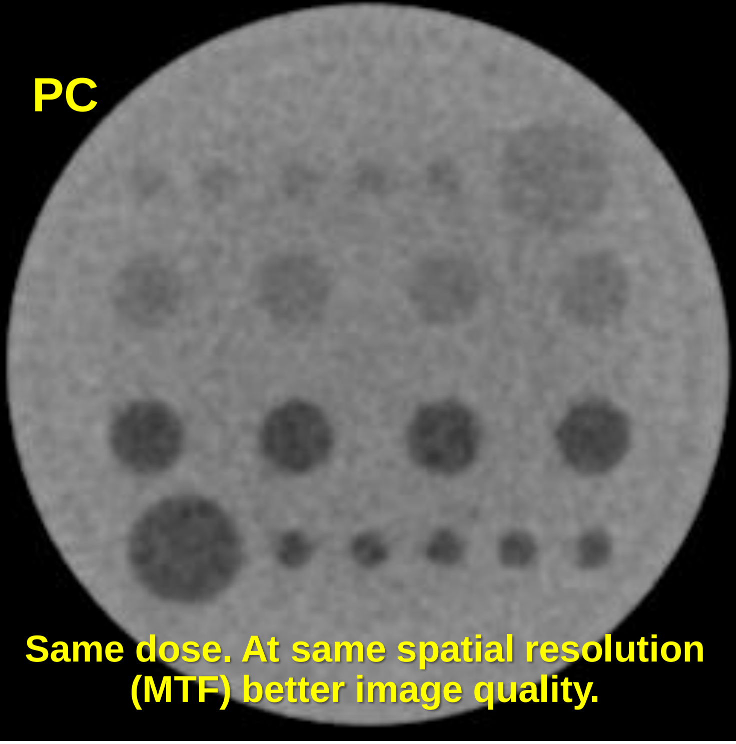

Same dose. At same spatial resolution (MTF) better image quality.

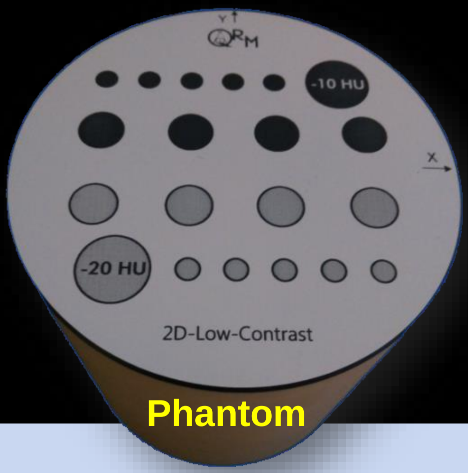

Phantom

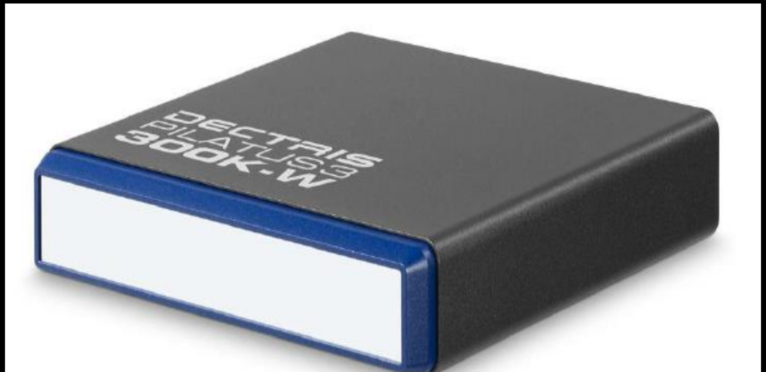

Photon Counting Detector

C = 0 HU, W = 80 HU

dkfz.

Indirect Conversion

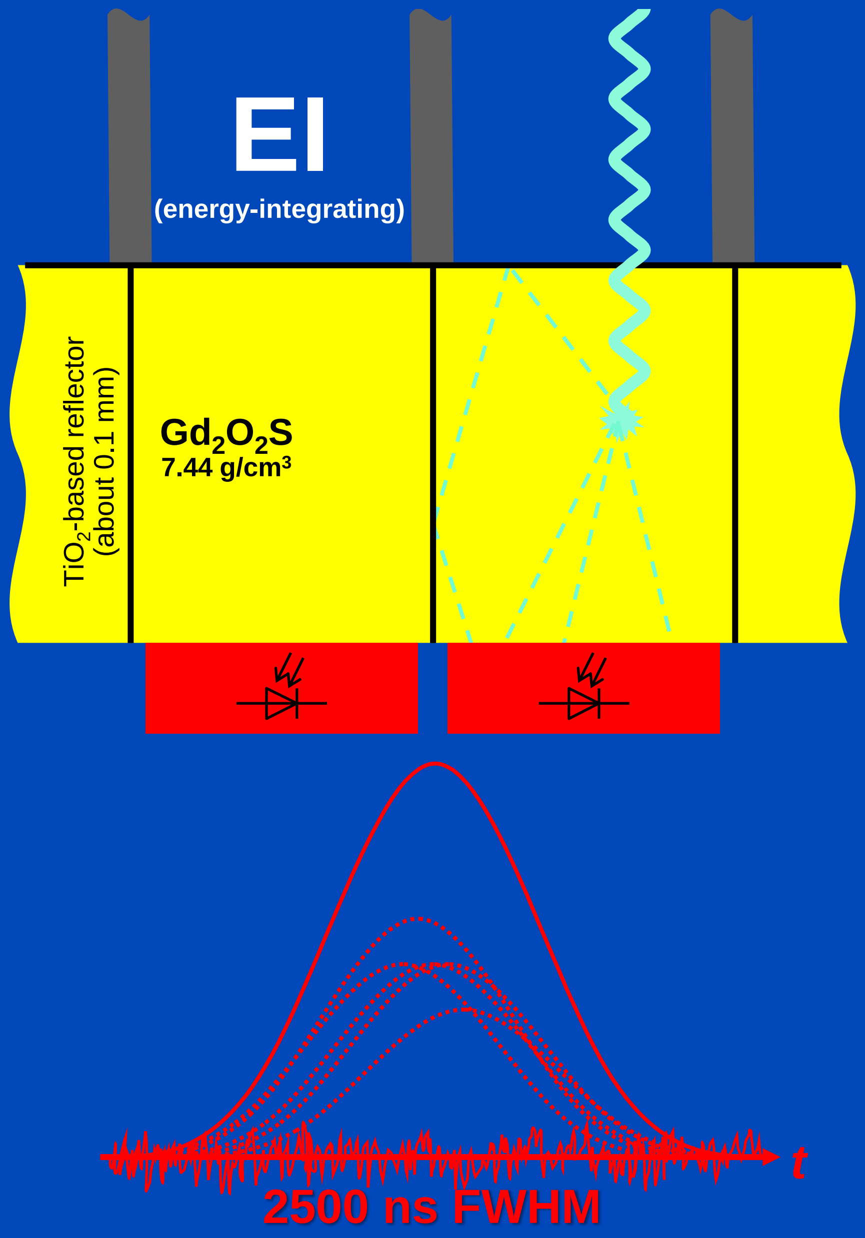

i.e. max O(40·10³) cps

Direct Conversion

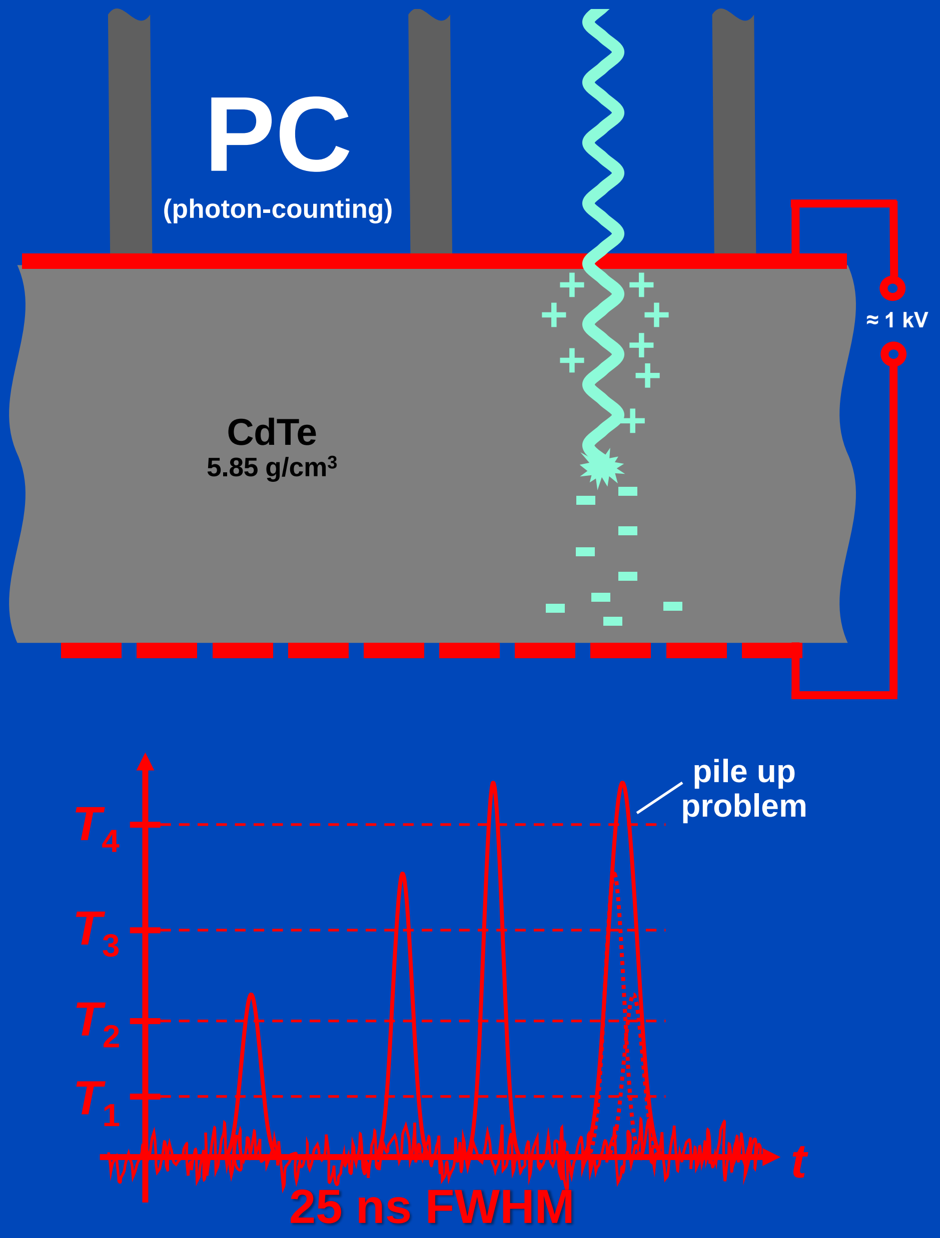

i.e. max O(40·10⁶) cps

Requirements for CT: up to 10^9 x-ray photon counts per second per mm^2.
Hence, photon counting only achievable for direct converters.

dkfz.

Energy-Selective Detectors: Improved Spectroscopy, Reduced Dose?

Ideally, bin spectra do not overlap, …

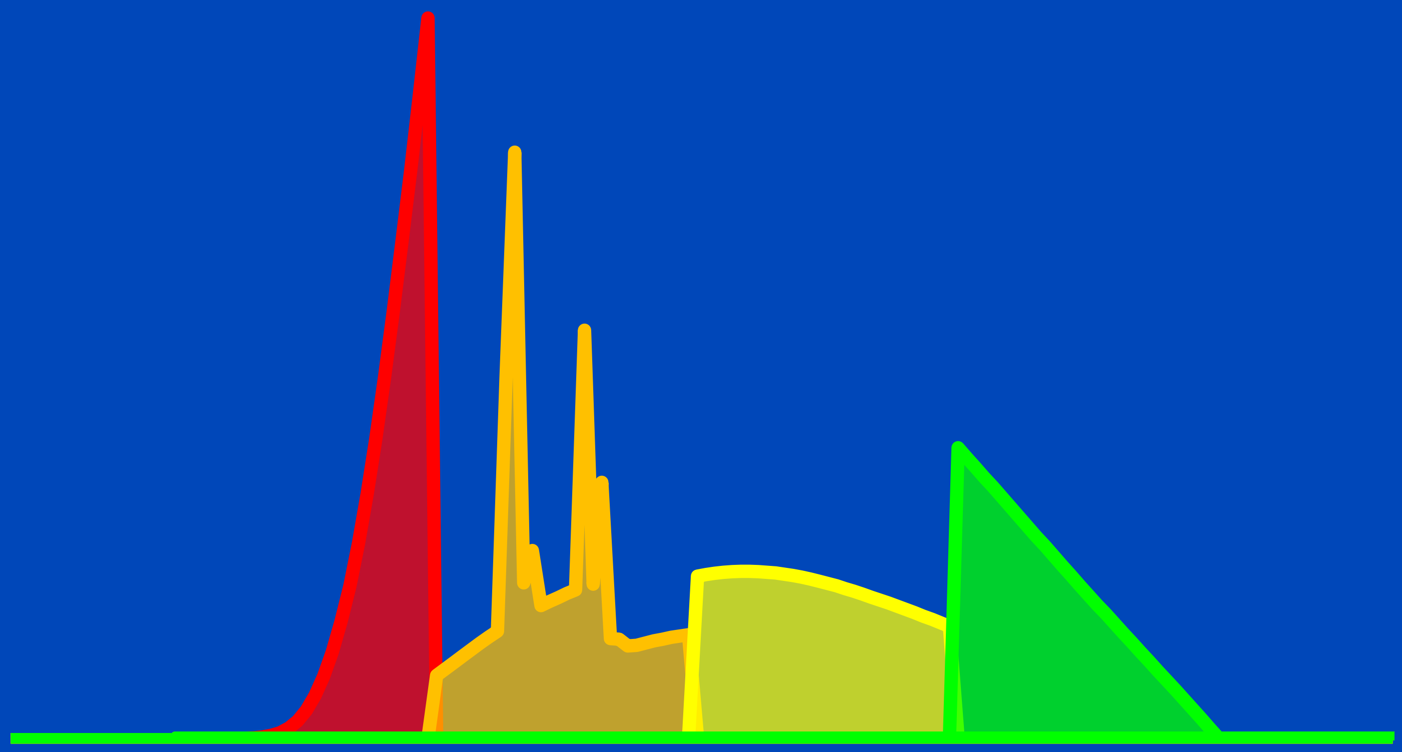

Spectra as seen with 4 bins after having passed a 32 cm water layer.

Energy-Selective Detectors: Improved Spectroscopy, Reduced Dose?

… realistically, however, they do!

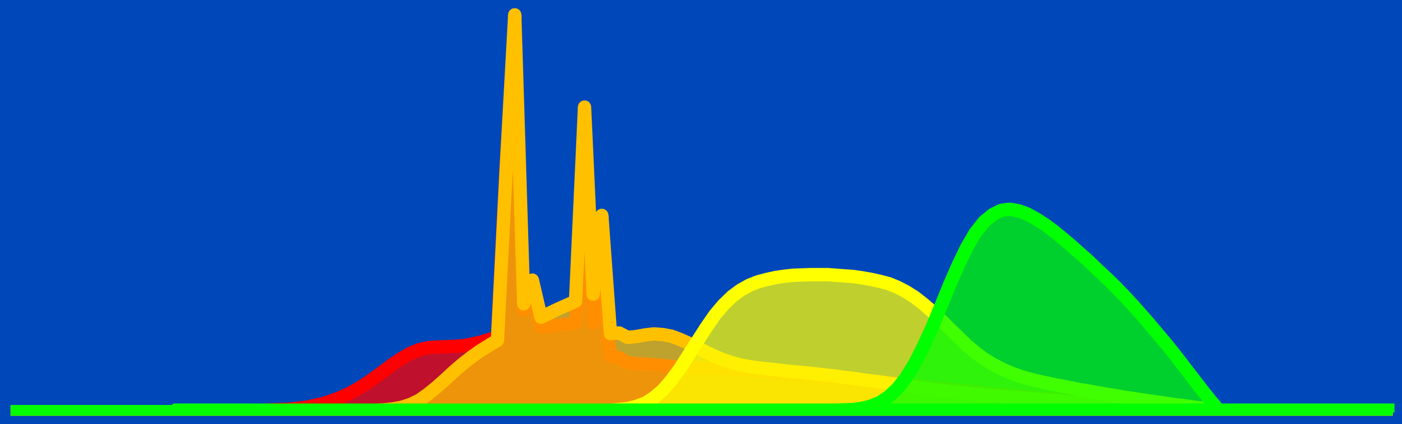

Spectra as seen with 4 bins after having passed a 32 cm water layer.

Photon Events

- Detection process in the sensor
- Photoelectric effect (e.g. 80 keV)

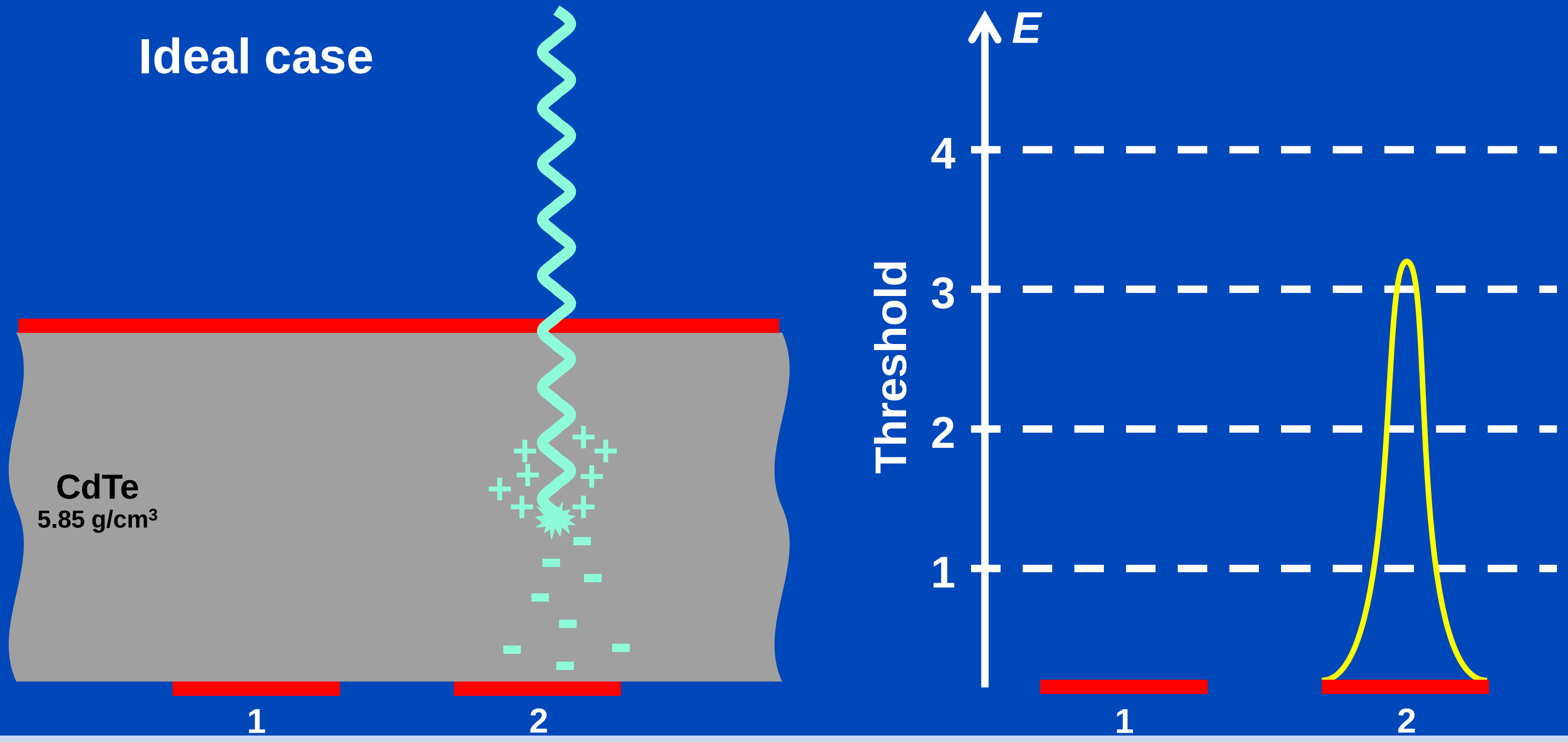

Photon Events

- Detection process in the sensor
- Compton scattering or K-fluorescence (e.g. 80 keV)

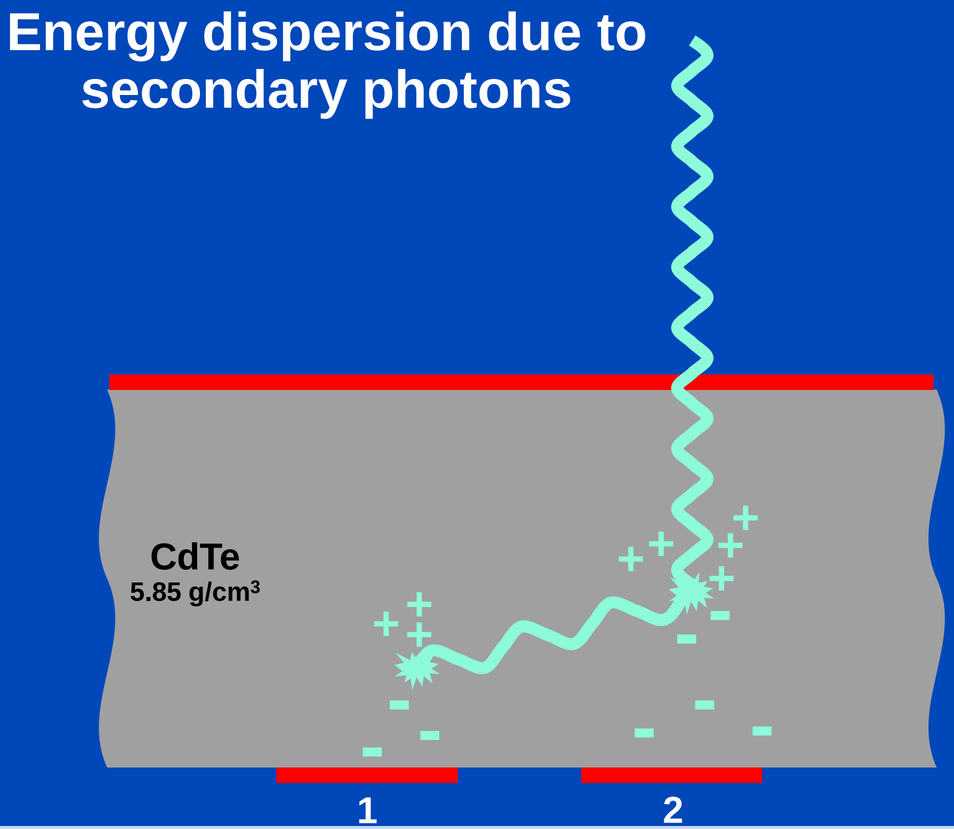

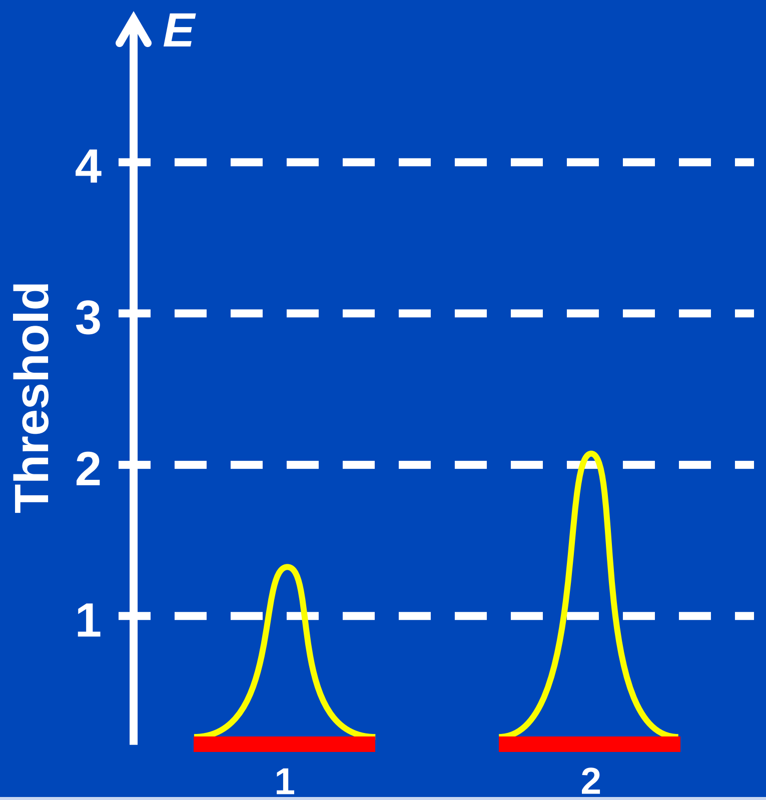

Photon Events

- Detection process in the sensor
- Photoelectric effect (e.g. 30 keV), charge sharing

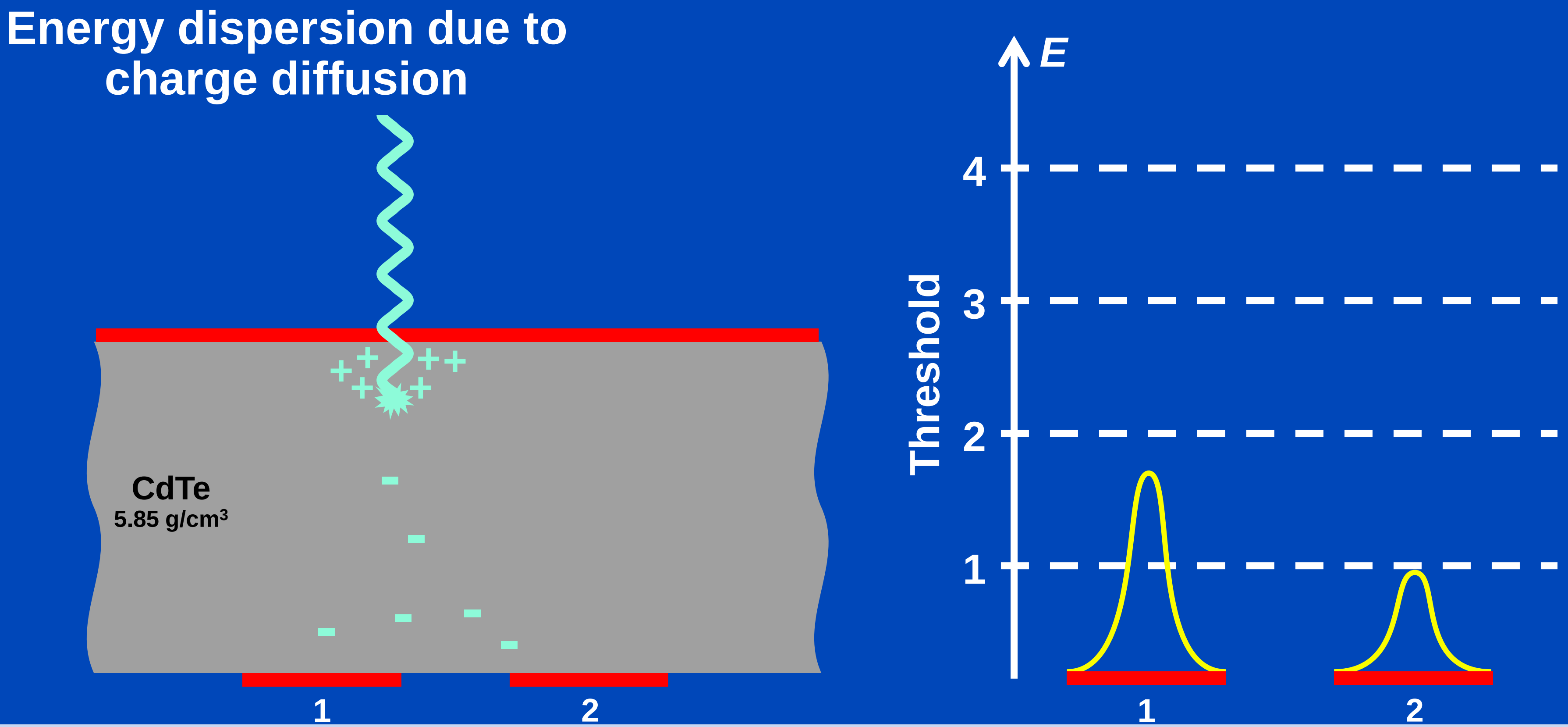

No Electronic Noise!

- Photon counting detectors have no electronic noise.
- Extreme low dose situations will benefit
  - Pediadric scans at even lower dose
  - Obese patients with less noise
  - Industrial CT with very long exposure times per frame
  - …

EI (Dexela)

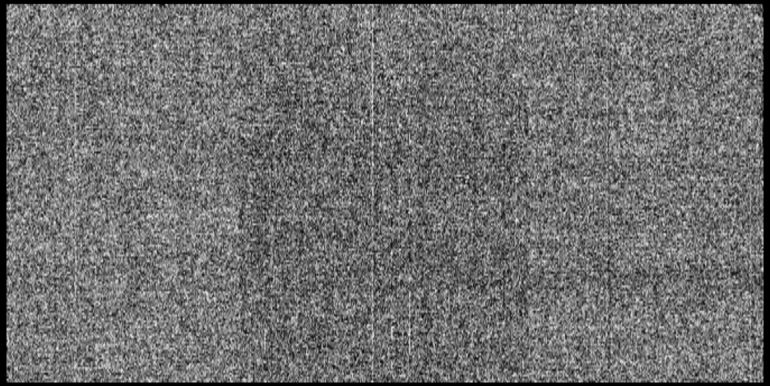

Readout noise only. Single events hidden!

PC (Dectris)

No readout noise. Single events visible!

18 frames, 5 min integration time per frame, x-ray off

Siemens Naeotom Alpha
The World‘s First Photon-Counting CT

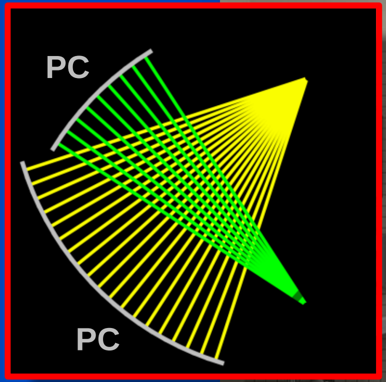

- **Tubes**
  - **tube A: 120 kW** } ≈ ¼ MW
  - **tube B: 120 kW**
  - **Focal spot size down to 181 µm**
- **Detectors**
  - **pixel size down to 150 µm**
  - **288 detector rows**
  - **2752 detector columns**
- **Speed**
  - **up to 4 rotations per second**
  - **up to 737 mm/s scan speed**
- **50 cm FOM**

Detector Pixel Force vs. Alpha

Force
920 × 96 detector pixels
pixel size 0.52 × 0.56 mm at iso
avg. sampling 0.56 × 0.6 mm at iso
57.6 mm z-coverage

Alpha (Quantum Plus)
1376 × 144 macro pixels
pixel size 0.3 × 0.352 mm at iso
avg. sampling 0.344 × 0.4 mm at iso
57.6 mm z-coverage

Alpha (UHR)
2752 × 120 pixels
pixel size 0.151 × 0.176 mm at iso
avg. sampling 0.172 × 0.2 mm at iso
24 mm z-coverage

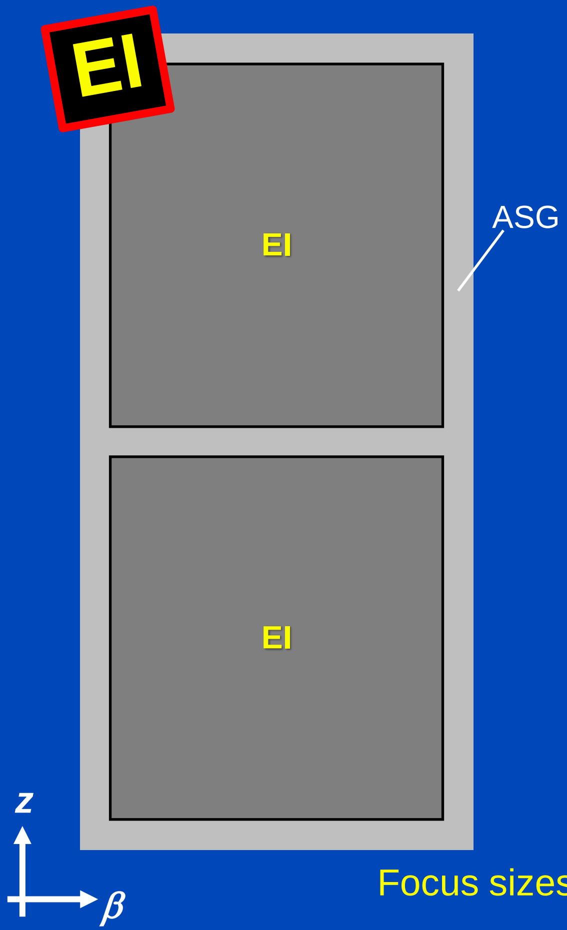

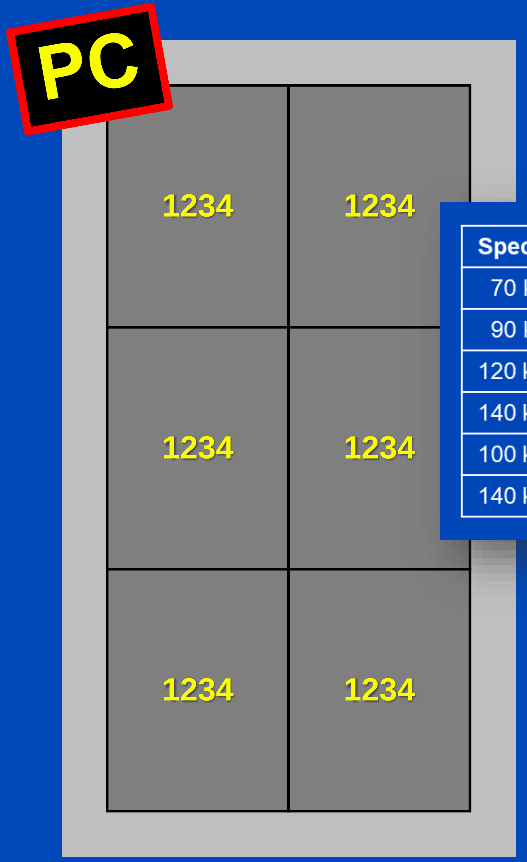

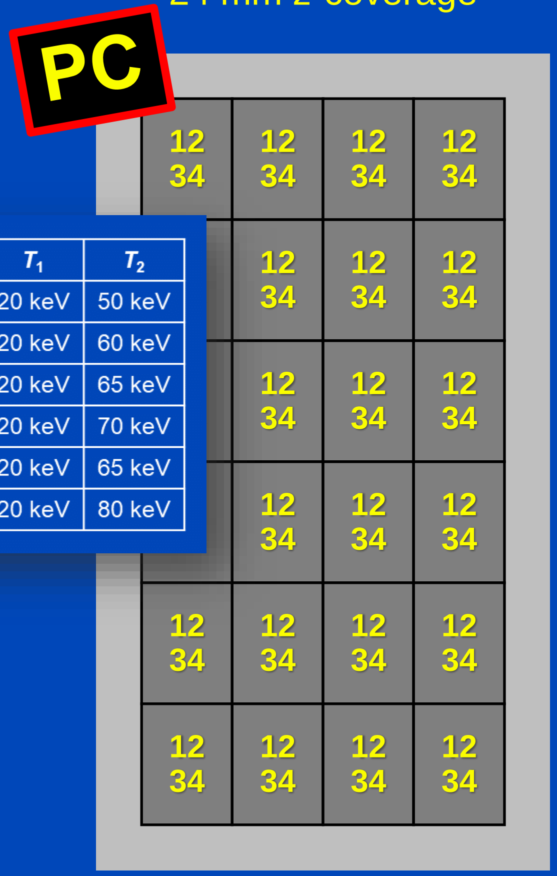

Spectrum	T_1	T_2
70 kV	20 keV	50 keV
90 kV	20 keV	60 keV
120 kV	20 keV	65 keV
140 kV	20 keV	70 keV
100 kV Sn	20 keV	65 keV
140 kV Sn	20 keV	80 keV

Focus sizes (Vectron): 0.181×0.226 mm, 0.271×0.7316 mm, 0.362×0.497 mm at iso
which are 0.4×0.5 mm, 0.6×0.7 mm, 0.8×1.1 mm at focal spot

ASG information taken from [J. Ferda et al. Computed tomography with a full FOV photon-counting detector in a clinical setting, the first experience. European Journal of Radiology 137:109614, 2021]

dkfz.

The “Small Pixel Effect”

or “To Bin or not to Bin?”

This nice phrase was coined by Prof. Norbert Pelc, Stanford University.

Avoid binning, if possible!

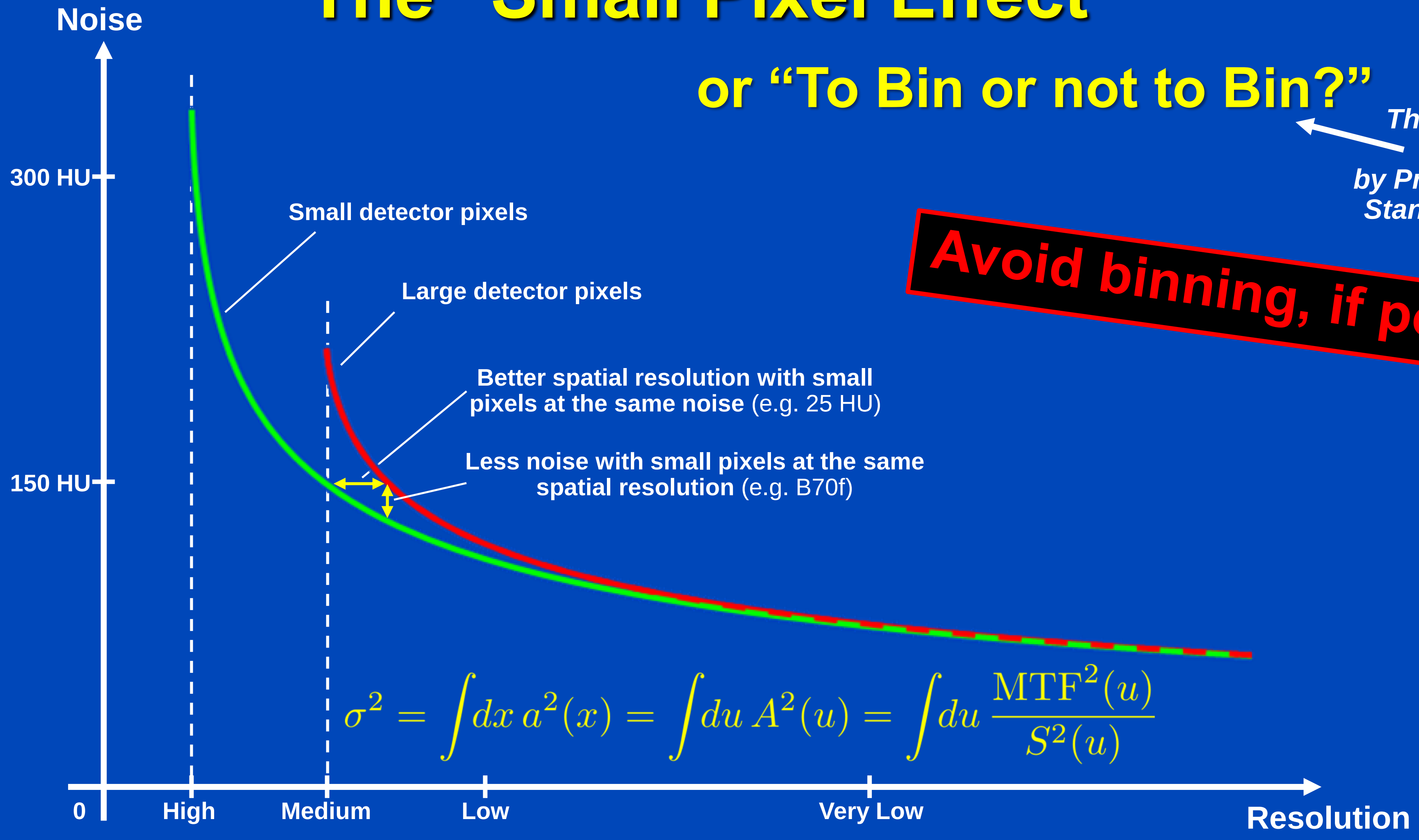

$$\sigma^2 = \int dx\, a^2(x) = \int du\, A^2(u) = \int du\, \frac{\mathrm{MTF}^2(u)}{S^2(u)}$$

Kachelrieß, Kalender. Med. Phys. 32(5):1321-1334, May 2005

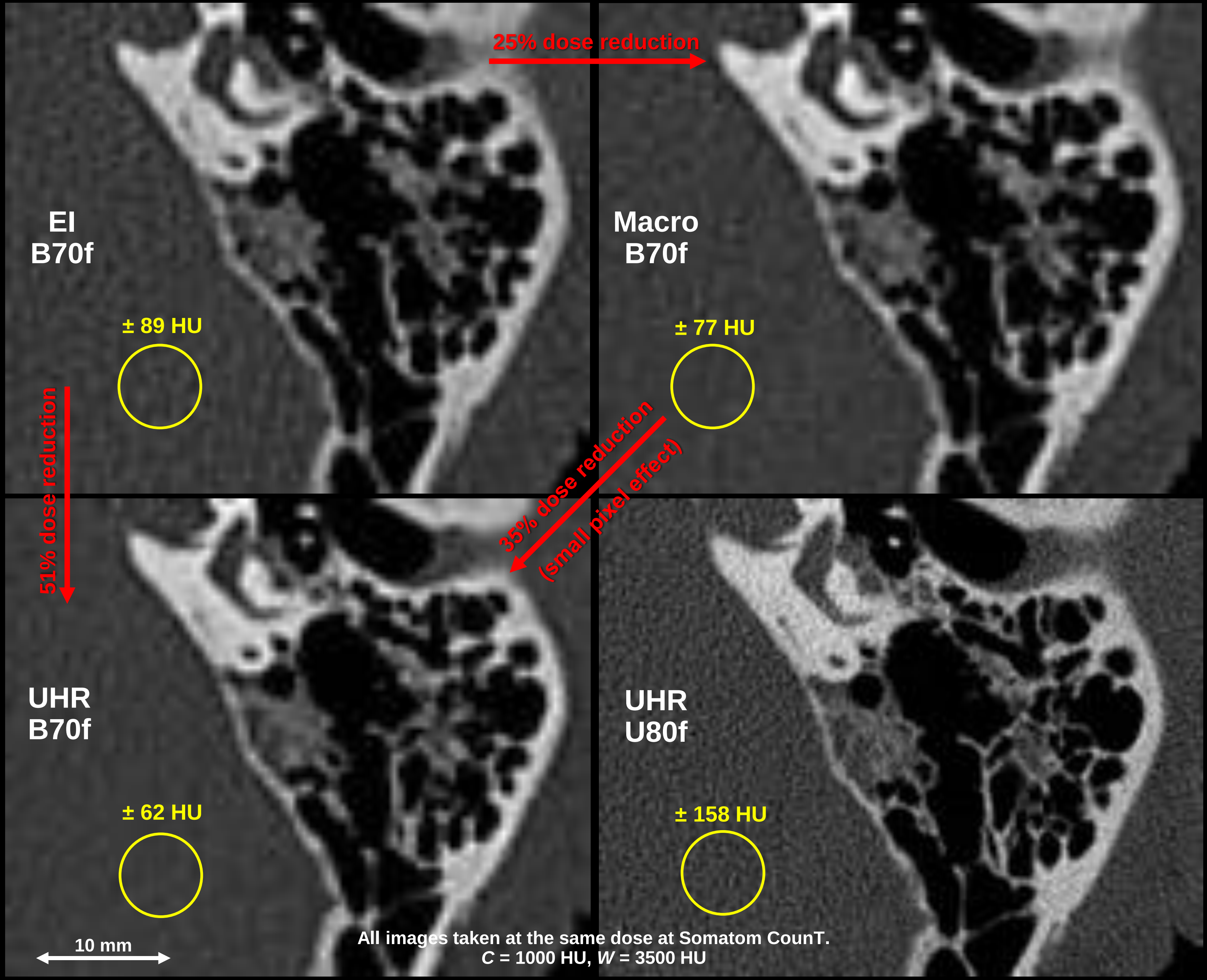

All images taken at the same dose at Somatom CounT.
C = 1000 HU, W = 3500 HU

Photon Counting used to Maximize CNR

- With PC, energy bin sinograms can be weighted individually, i.e. by a weighted summation.
- To optimize the CNR the optimal bin weighting factor w_b is given by (weighting after log):

$$w_b \propto \frac{C_b}{V_b}$$

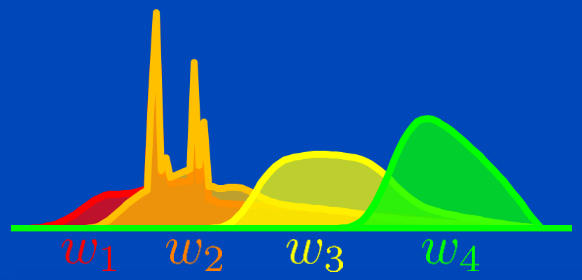

- The resulting CNR is

$$\mathrm{CNR}^2 = \frac{\left(\sum_b w_b C_b\right)^2}{\sum_b w_b^2 V_b}$$

- At the optimum this evaluates to

$$\mathrm{CNR}^2 = \sum_{b=1}^{B} \mathrm{CNR}_b^2$$

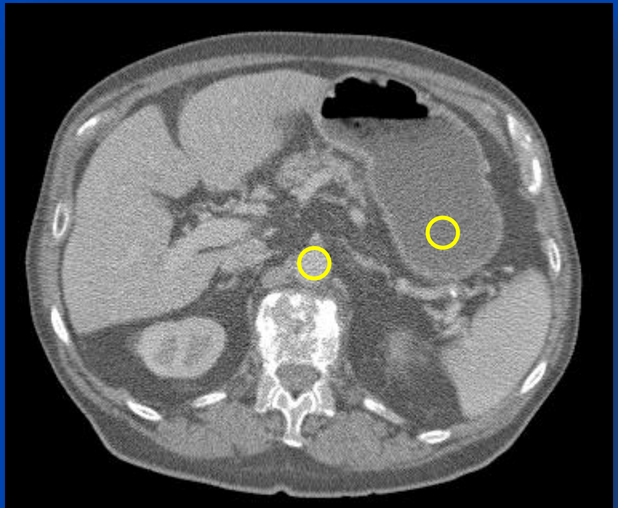

The two ROIs are used to measure the CNR.

Material Decomposition or CNR Maximization?

- W = soft tissue (water) signal, X = iodine signal
- Assume same noise N, e.g. 50 HU, in both bin measurements M_1 and M_2
  - Var M_1 = Var M_2 = N^2 regardless of whether iodine is present or not
- PCCT measurement
  - Measurement 1 (high bin): $M_1 = W + 0.25\,X$ — $\mathrm{CNR}^2 = X^2 / 16\,N^2$
  - Measurement 2 (low bin): $M_2 = W + 0.5\,X$ — $\mathrm{CNR}^2 = X^2 / 4\,N^2$
- Material decomposition
  - Estimated iodine: $4\,(M_2 - M_1)$ — Variance = 16 (Var M_2 + Var M_1) = $32\,N^2$ — $\mathrm{SNR}^2 = X^2 / 32\,N^2$
  - Estimated soft tissue: $2\,M_1 - M_2$ — Variance = 4 Var M_1 + Var M_2 = $5\,N^2$ — $\mathrm{SNR}^2 = W^2 / 5\,N^2$
- CNR maximization
  - Compute $(1 - w)\,M_1 + w\,M_2$ — Variance = $(1 - w)^2\,N^2 + w^2\,N^2 = (1 - 2\,w + 2\,w^2)\,N^2$
  - Iodine value minus soft tissue value = Contrast = $(1 - w)\,0.25\,X + w\,0.5\,X$
  - Maximizing CNR yields $w = 2/3$ — $\mathrm{CNR}^2 = 5\,X^2 / 16\,N^2$

This simple toy example assumes iodine to contribute half as much to the gray value for the high bin as for the low bin.
CNR refers to the contrast between iodine and soft tissue. SNR refers to the contrast between the decomposed material and air.

Linear Mixing Techniques

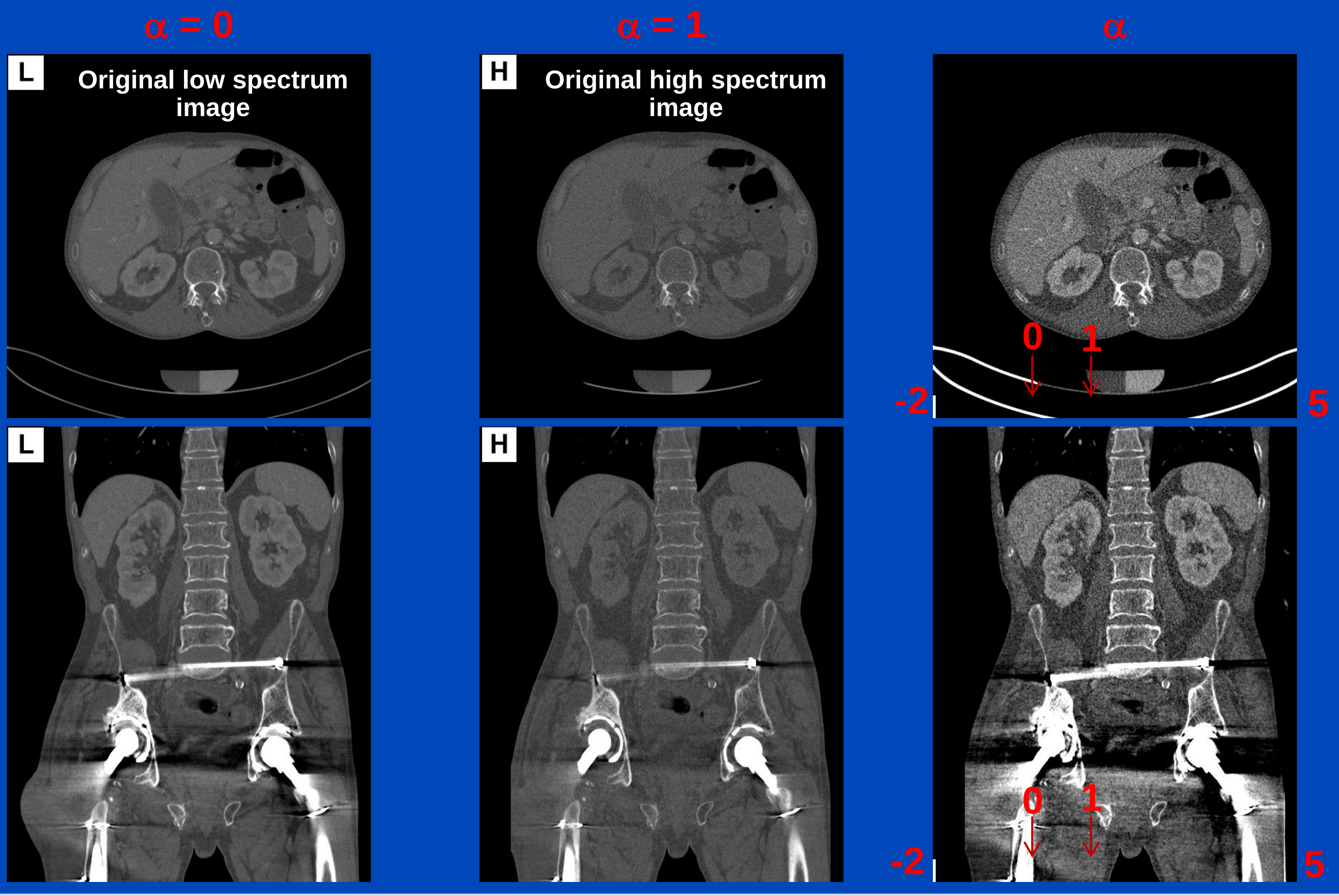

C = 300 HU, W = 1400 HU

Summary on PCCT

- Higher efficiency
  - better image quality
  - reduced measurement times
- No electronic noise
  - very long exposures possible
  - potential to overcome photon starvation
- Spectral information on demand
  - material discrimination
  - artifact reduction
  - combination with DECT acquisition possible and reasonable
- High frame rates also for off-the-shelve PC detectors
  - can be of interest for inspection tasks

ARTIFICIAL INTELLIGENCE

Deep RAR Examples

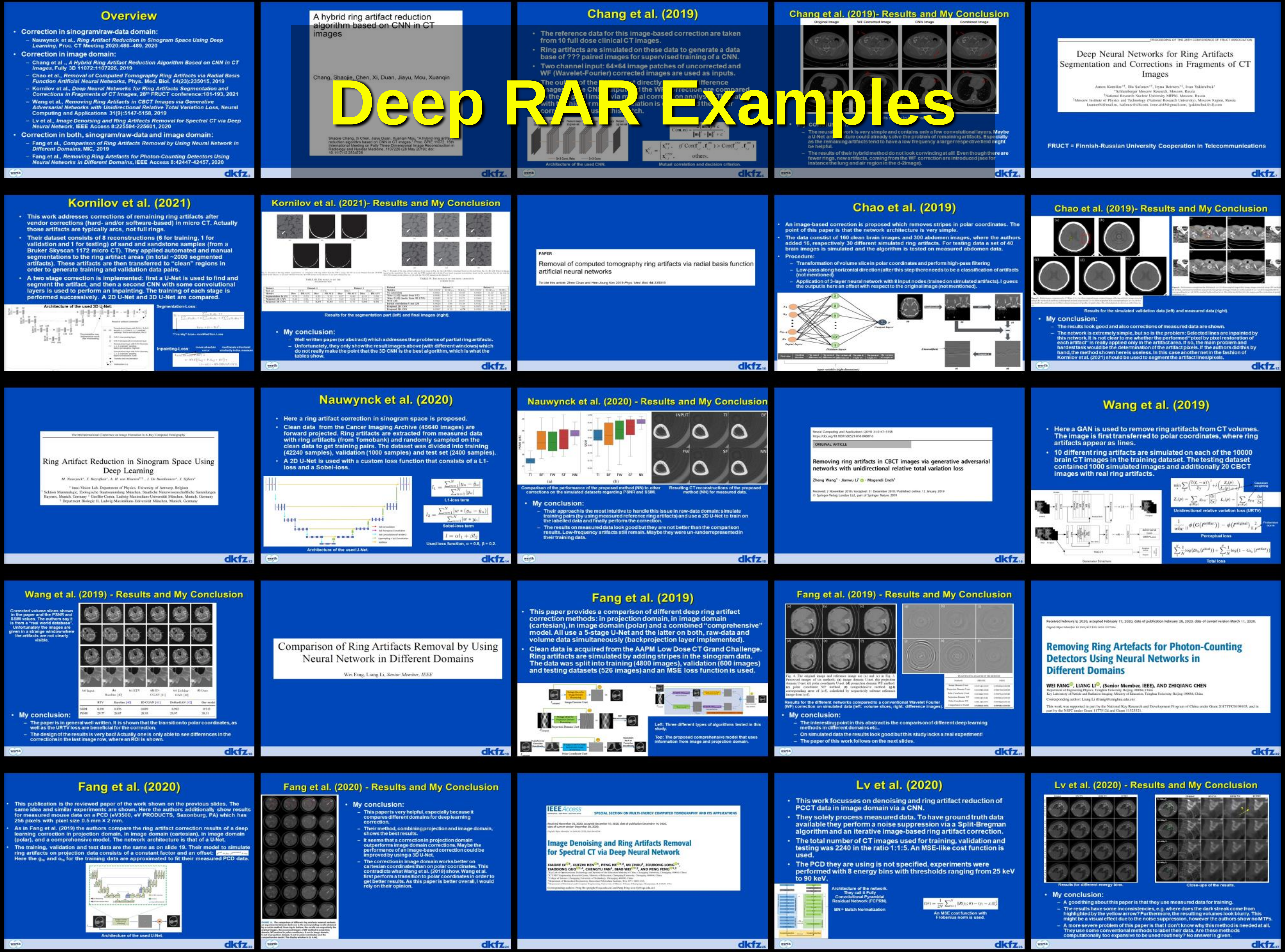

Deep Detruncation

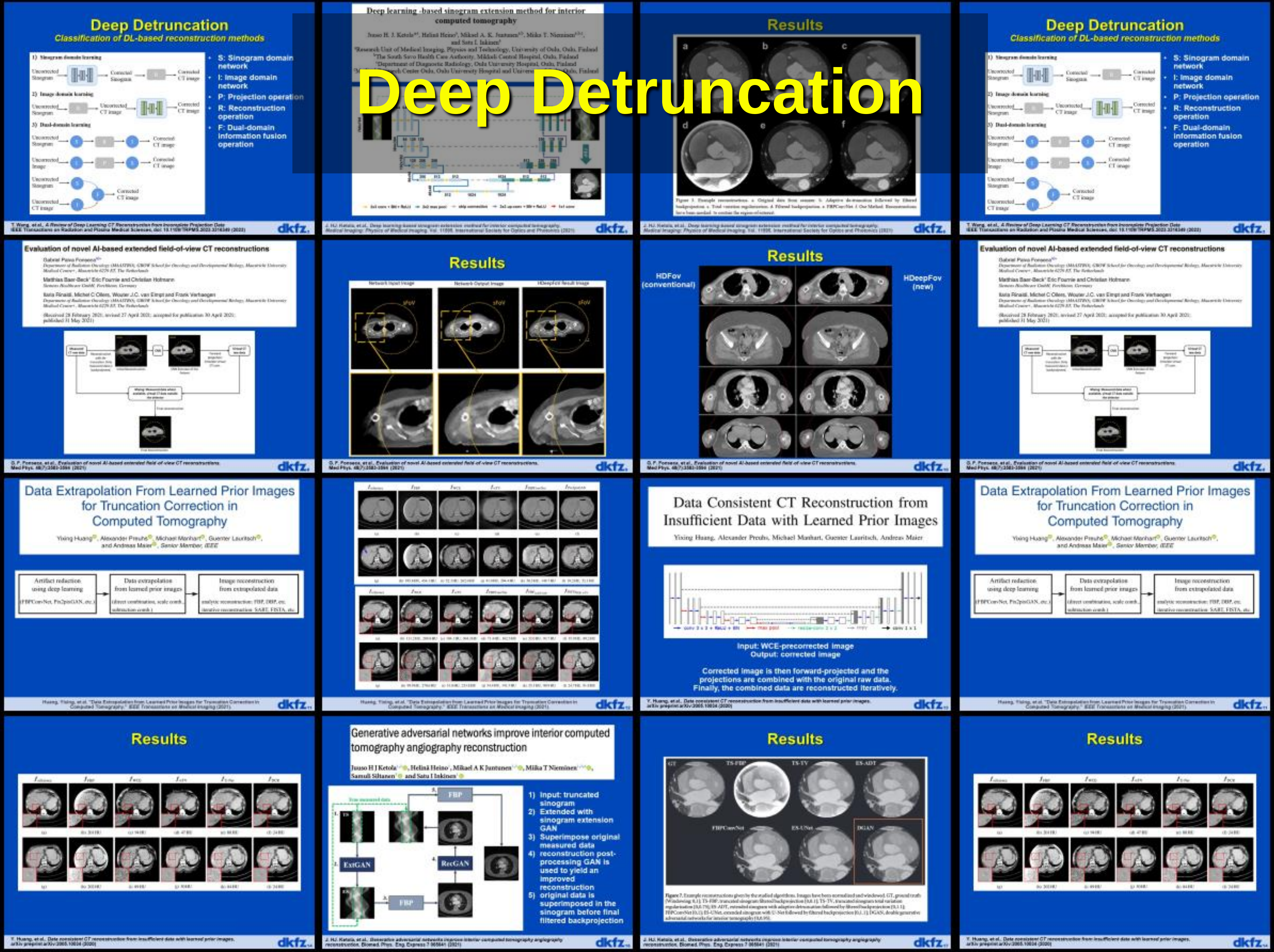

Deep MAR Examples

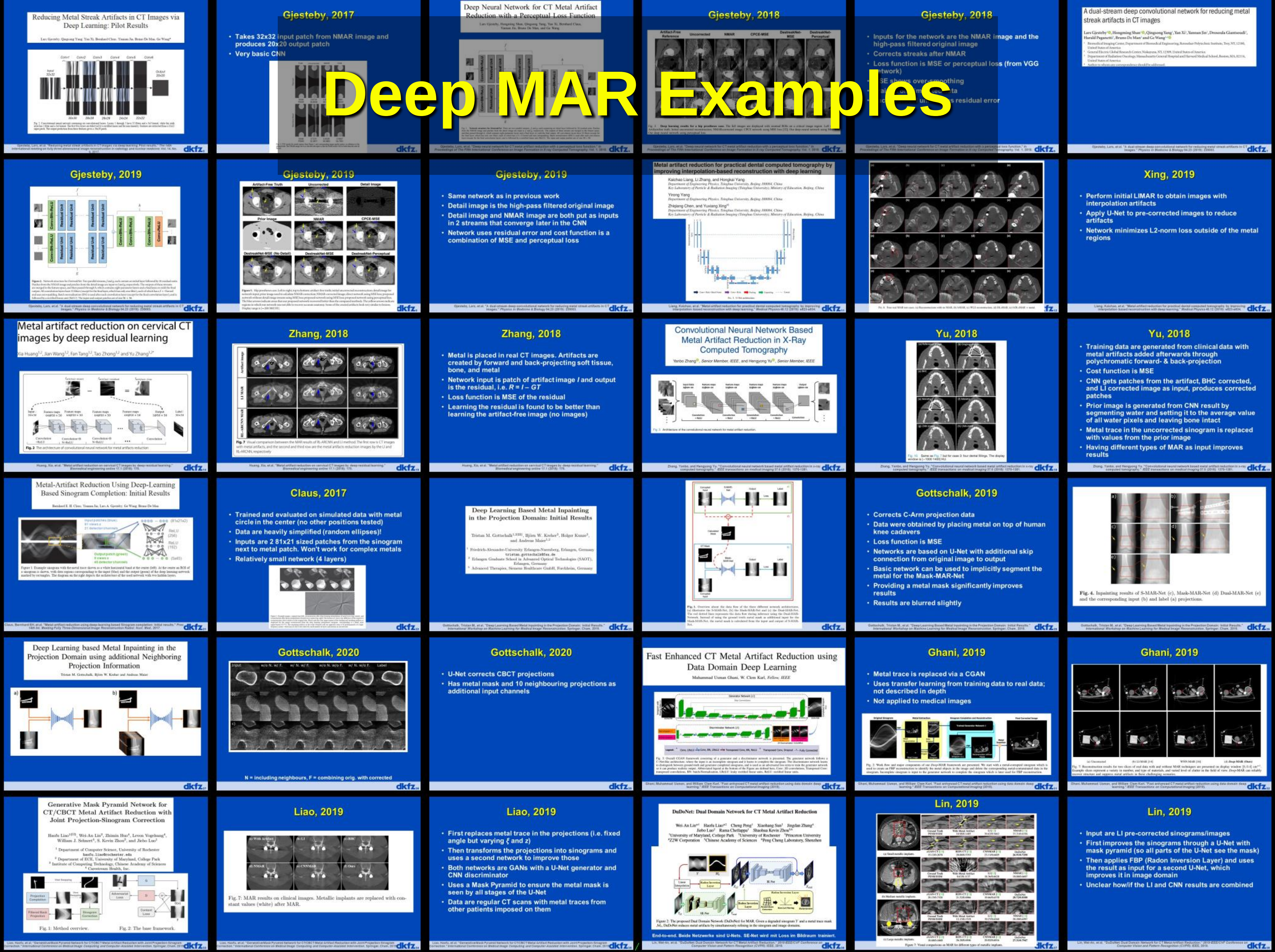

Deep MAR Examples

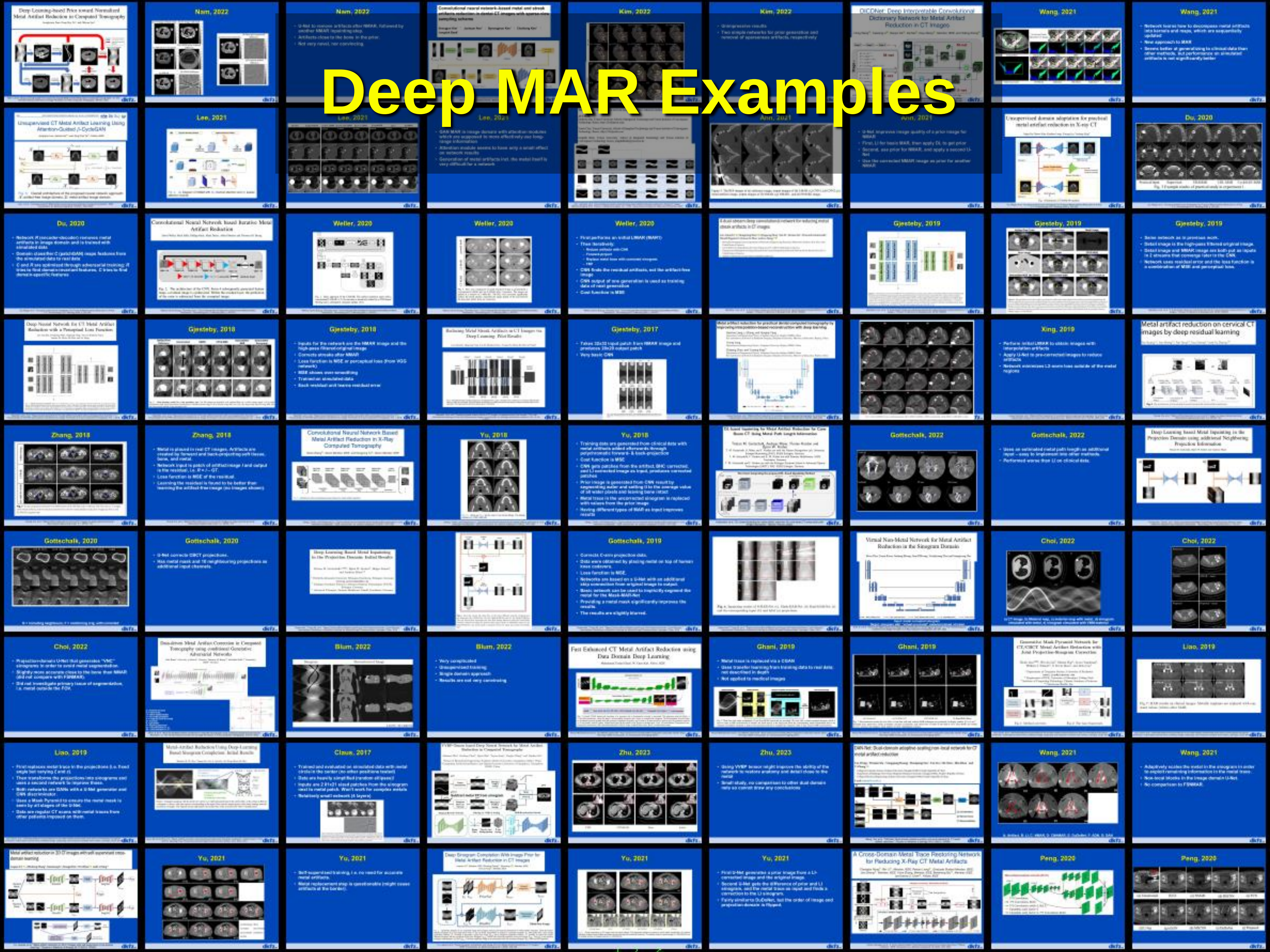

Sparse View Restoration Example

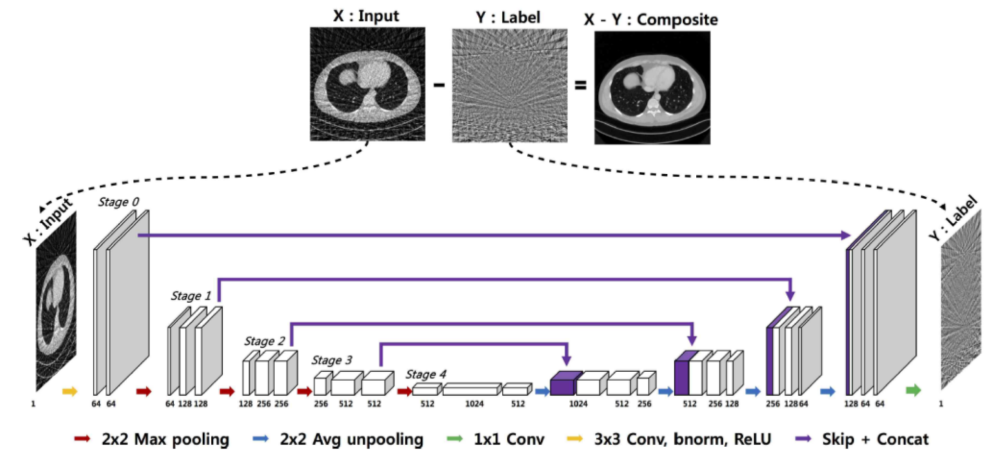

Figure 1. The proposed deep residual learning architecture for sparse view CT reconstruction.

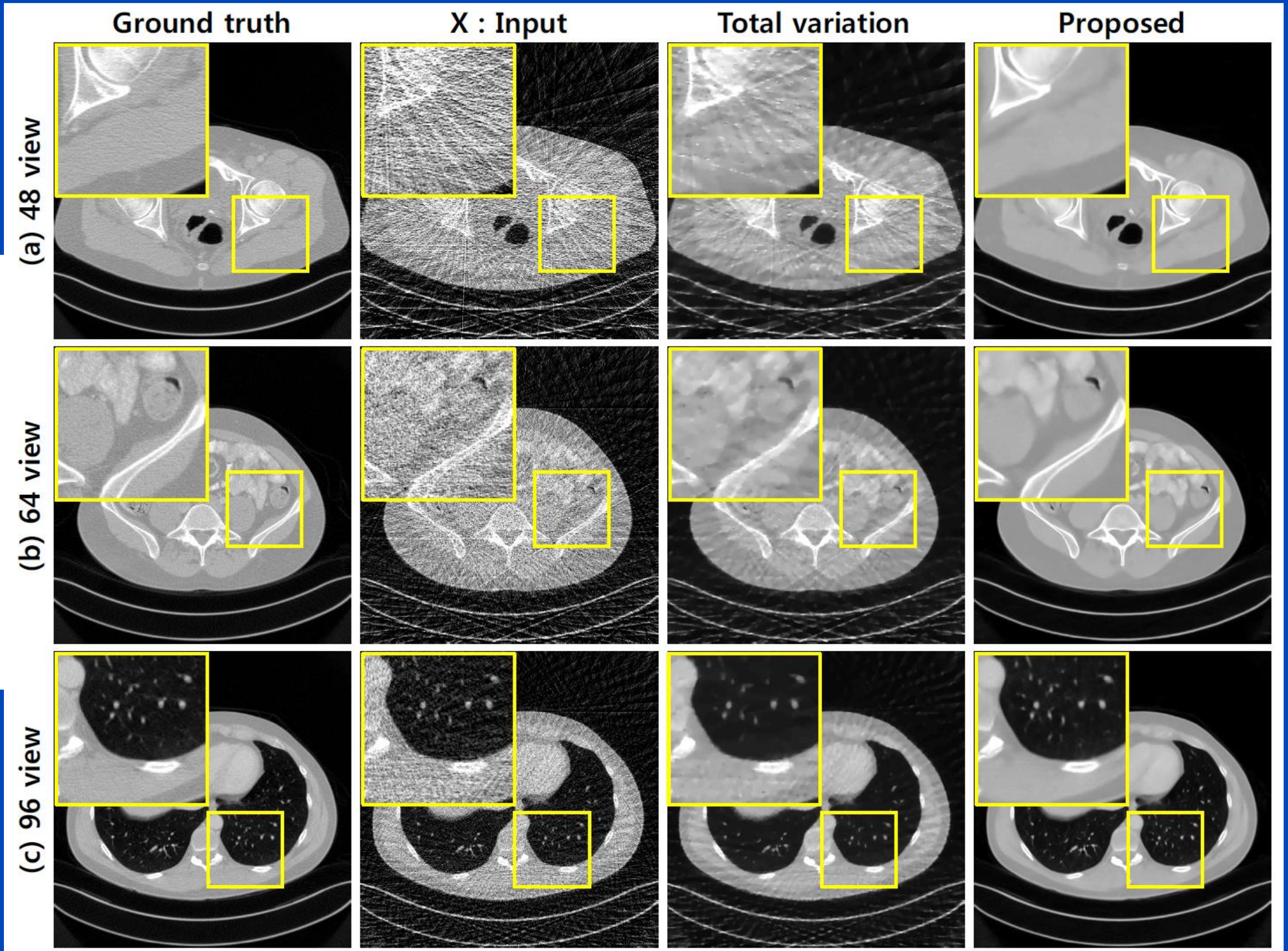

Yo Seob Han, Jaejun Yoo and Jong Chul Ye. Deep Residual Learning for Compressed Sensing CT Reconstruction via Persistent Homology Analysis. ArXiv 2016.

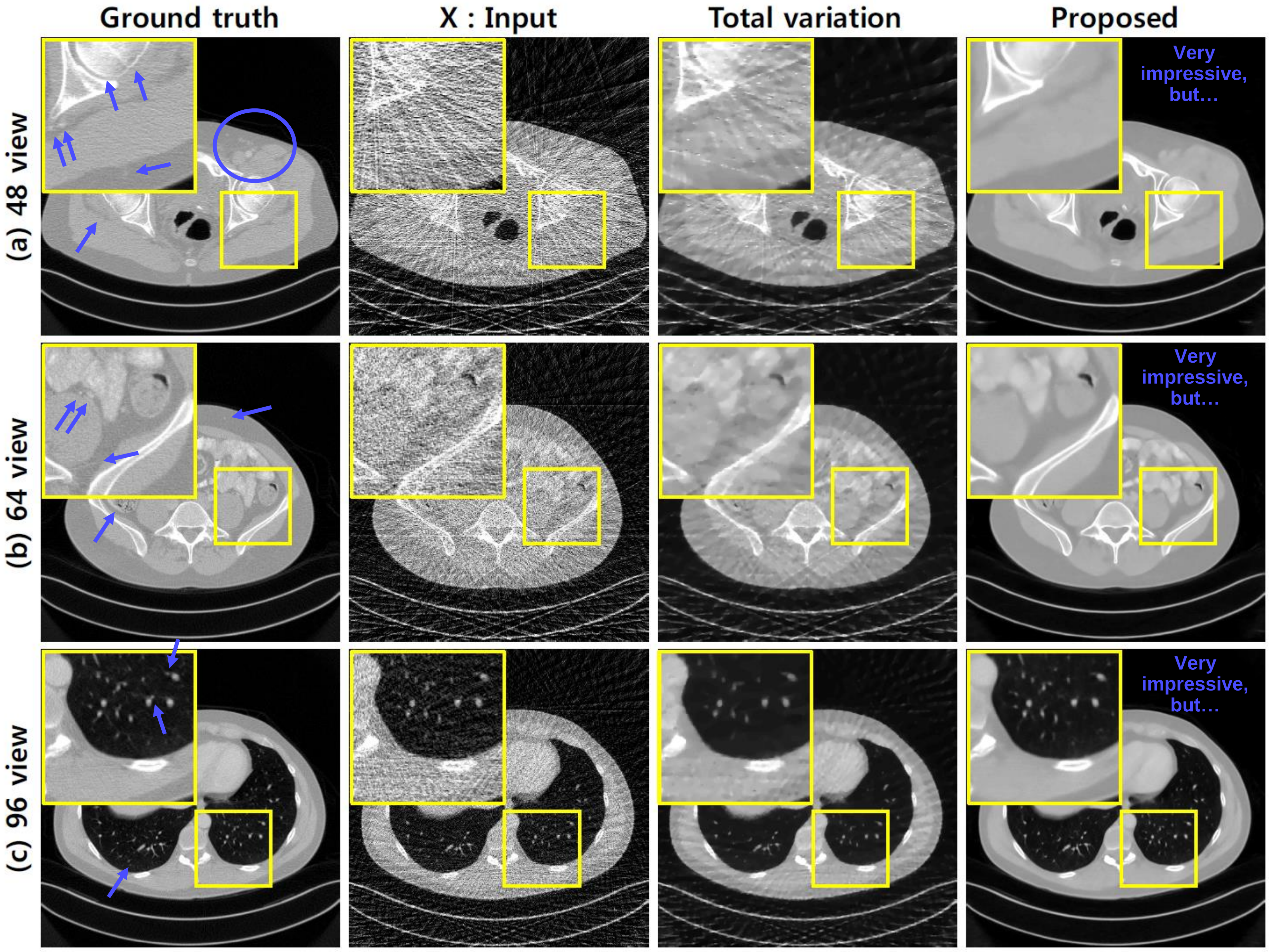
Ground truth
X : Input
Total variation
Proposed
(a) 48 view
(b) 64 view
(c) 96 view
Very impressive, but…
Very impressive, but…
Very impressive, but…

Component-Specific Denoising/Desparsifying

- We assume to have one long-acquisition scan of the component
- Generate training data via random transformations and deformations
- Generate datasets for training, validation and :
  - GT: Long-acquisition ground truth
  - UN: undersampled + noise reconstruction (80 projections, Poisson noise)
  - N: Noisy reconstruction (800 projections, with Poisson noise)

- Train three U-Nets
  - Sh-Unet-MSE: Shallow structure (3× downsampling, initial filter size: 16) with MSE
  - Unet-MSE: Deeper structure (4× downsampling, initial filter size: 16) with MSE
  - Unet-Adv: Deeper structure trained in WGAN-GP setting with perceptual and MSE component
- All networks are trained on patches of size 256^2 on the UN dataset

Results
Test Data (UN) · Sh-Unet-MSE

Input

Prediction

GT

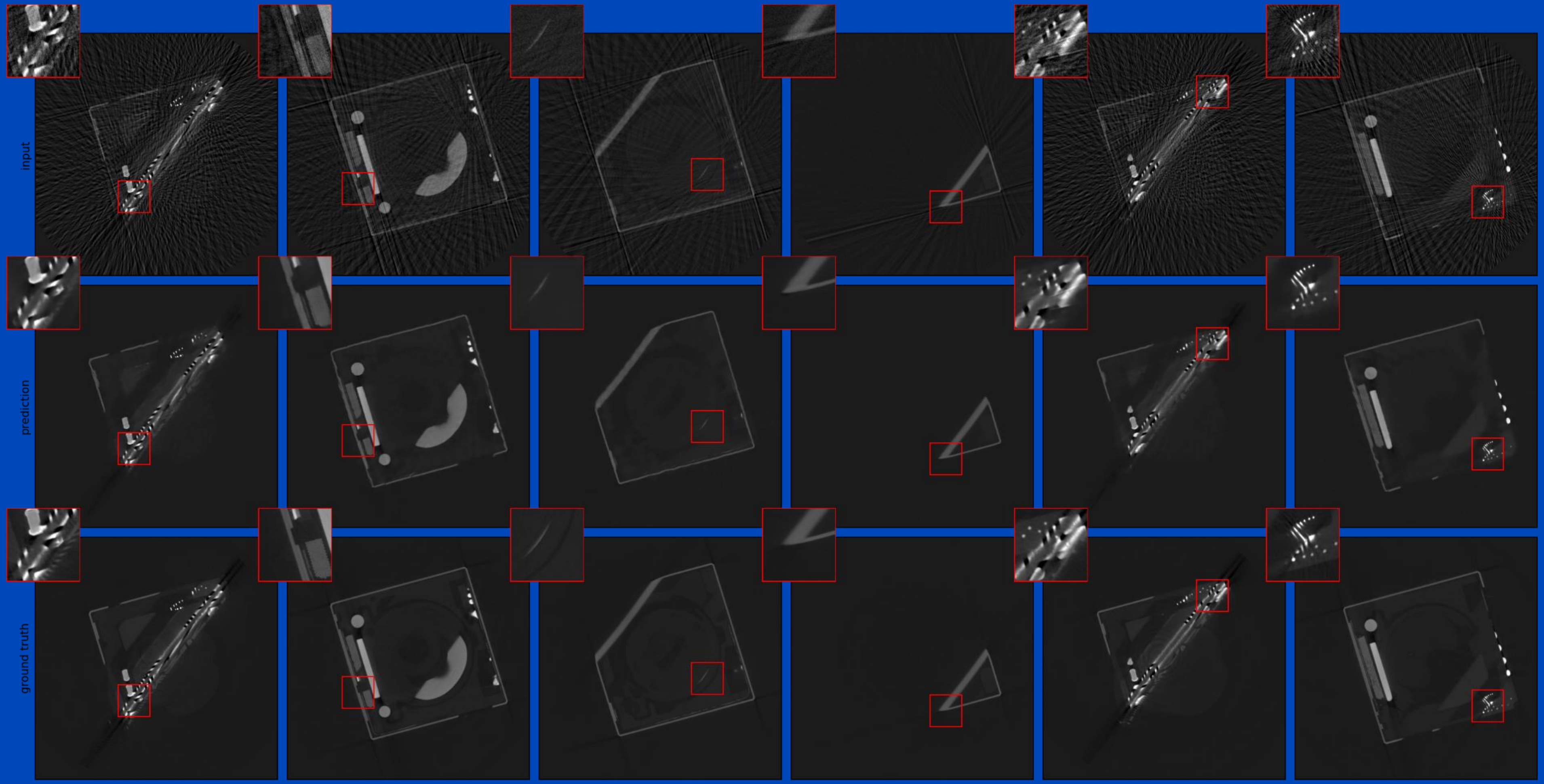

Ground Truth

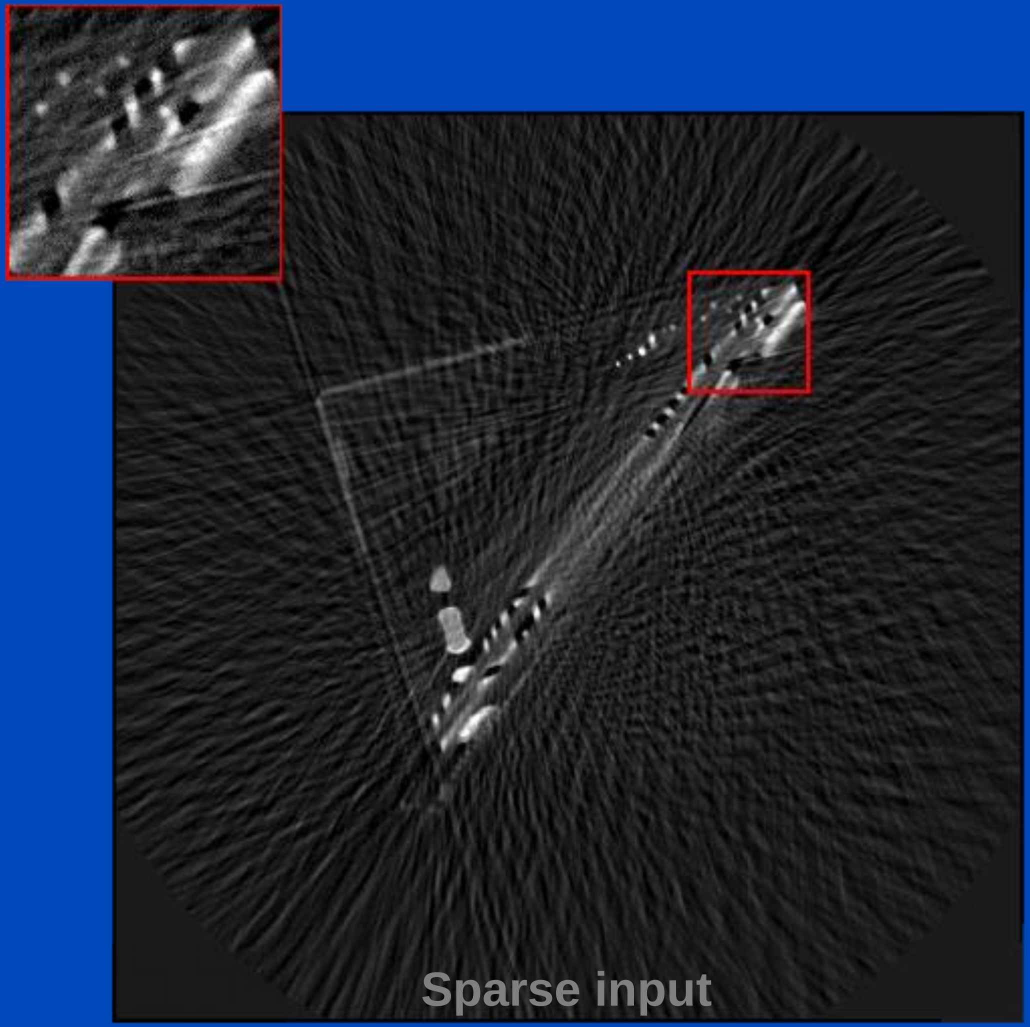

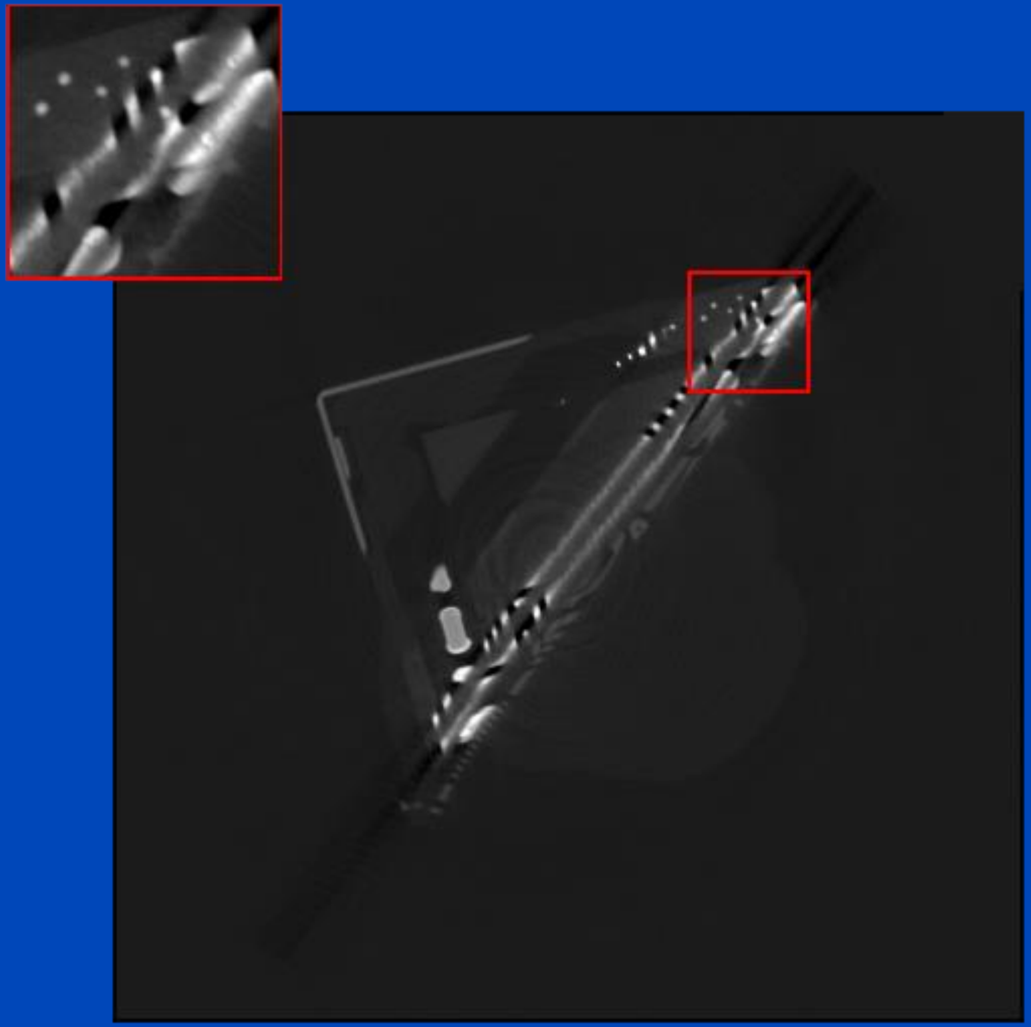

Shallow Unet

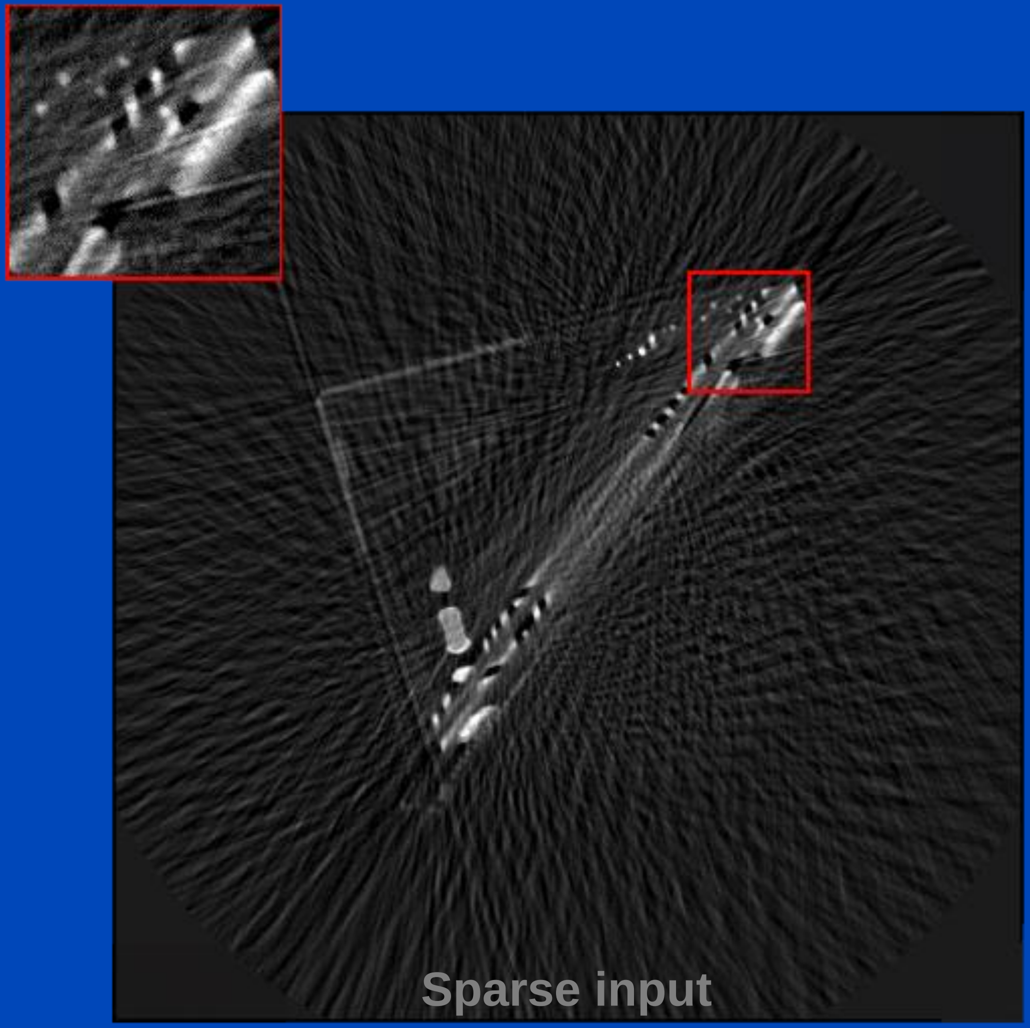

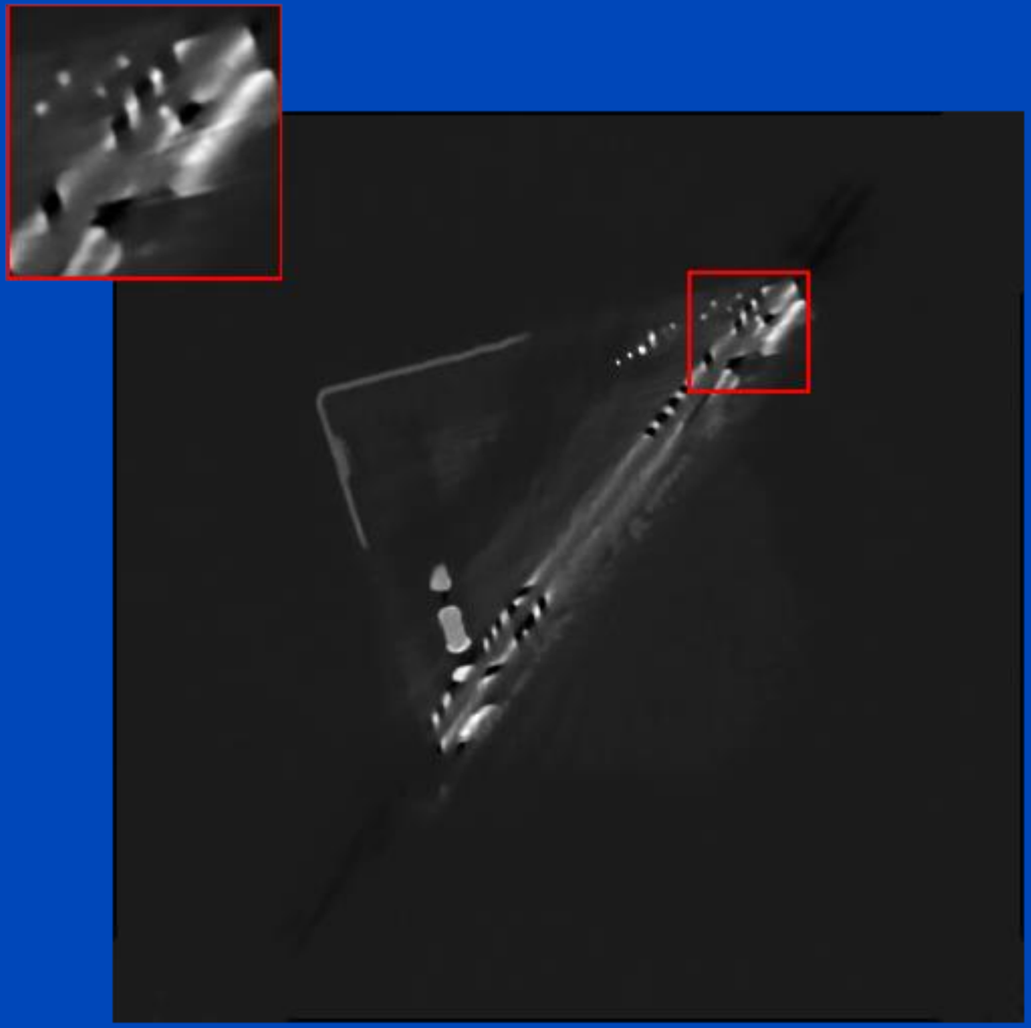

Deep Unet

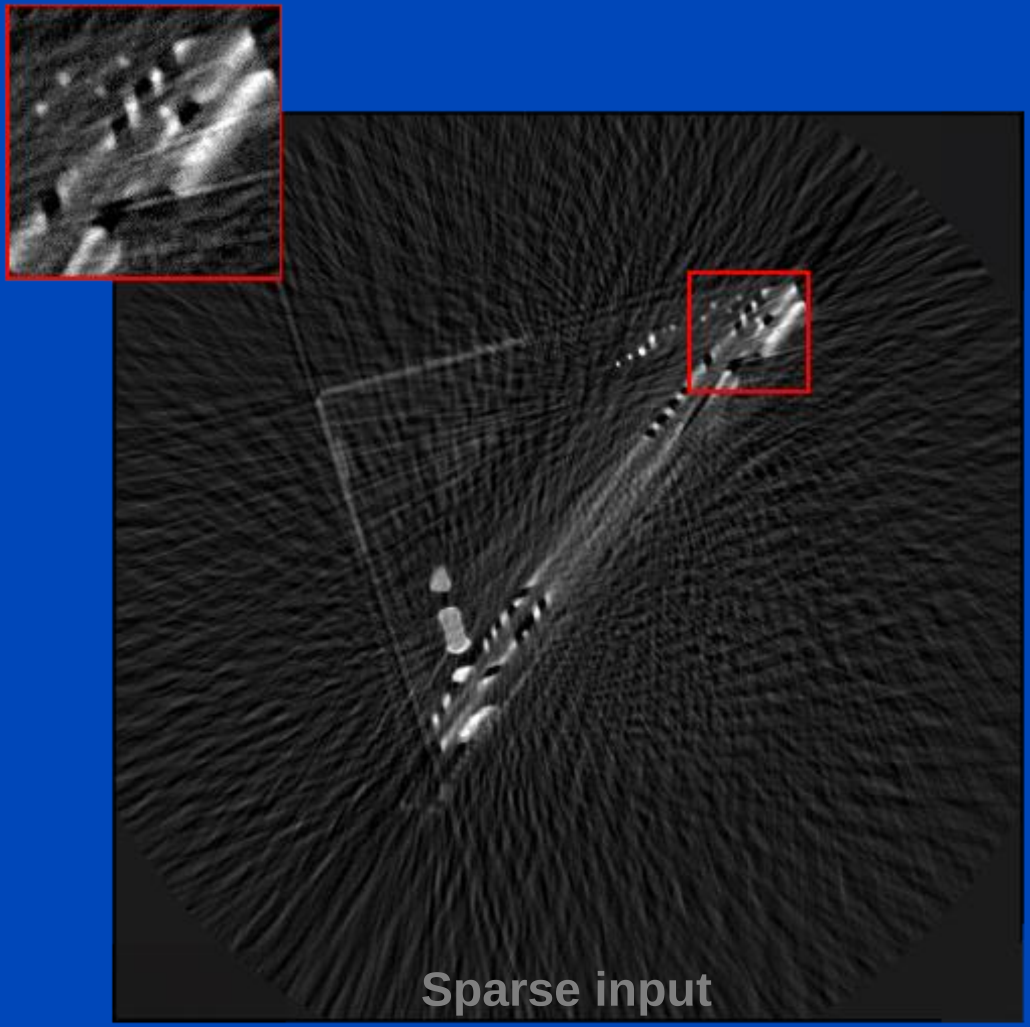

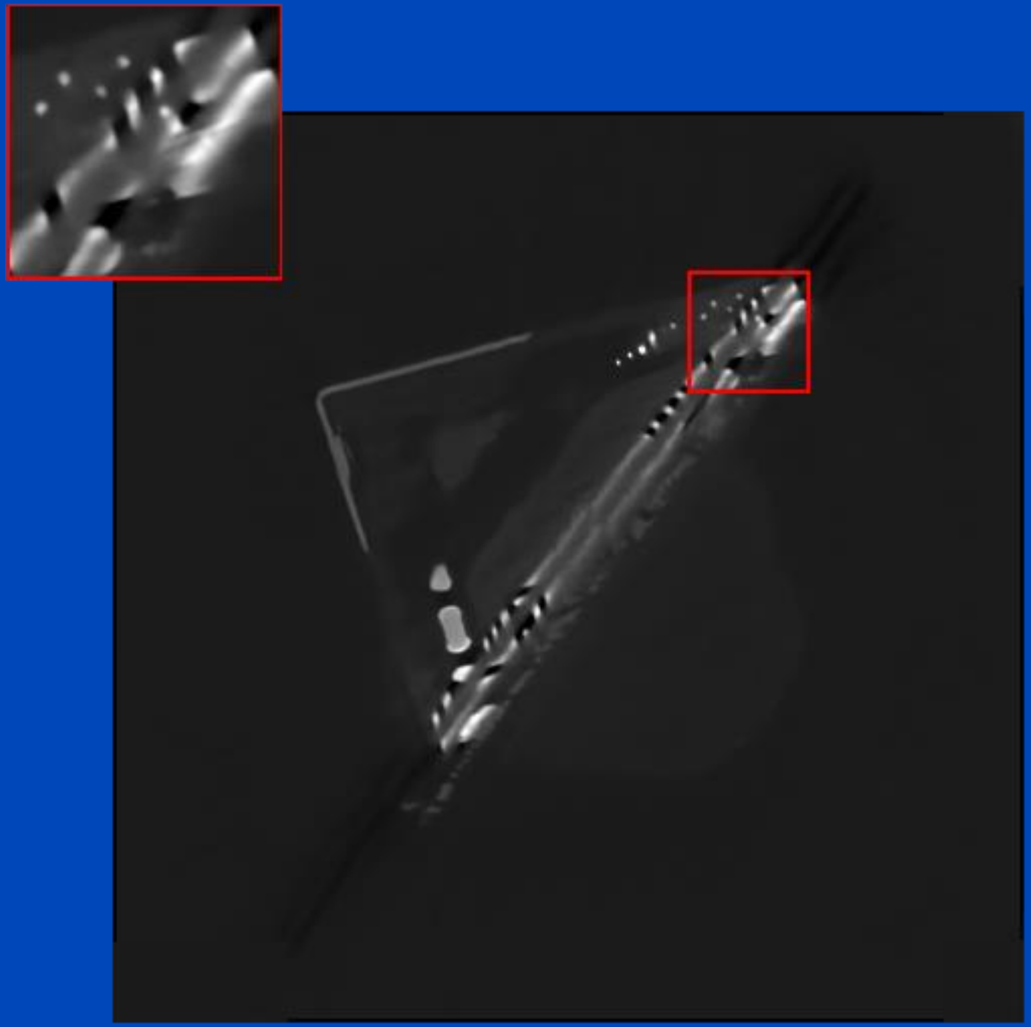

Deep Adversarial Unet

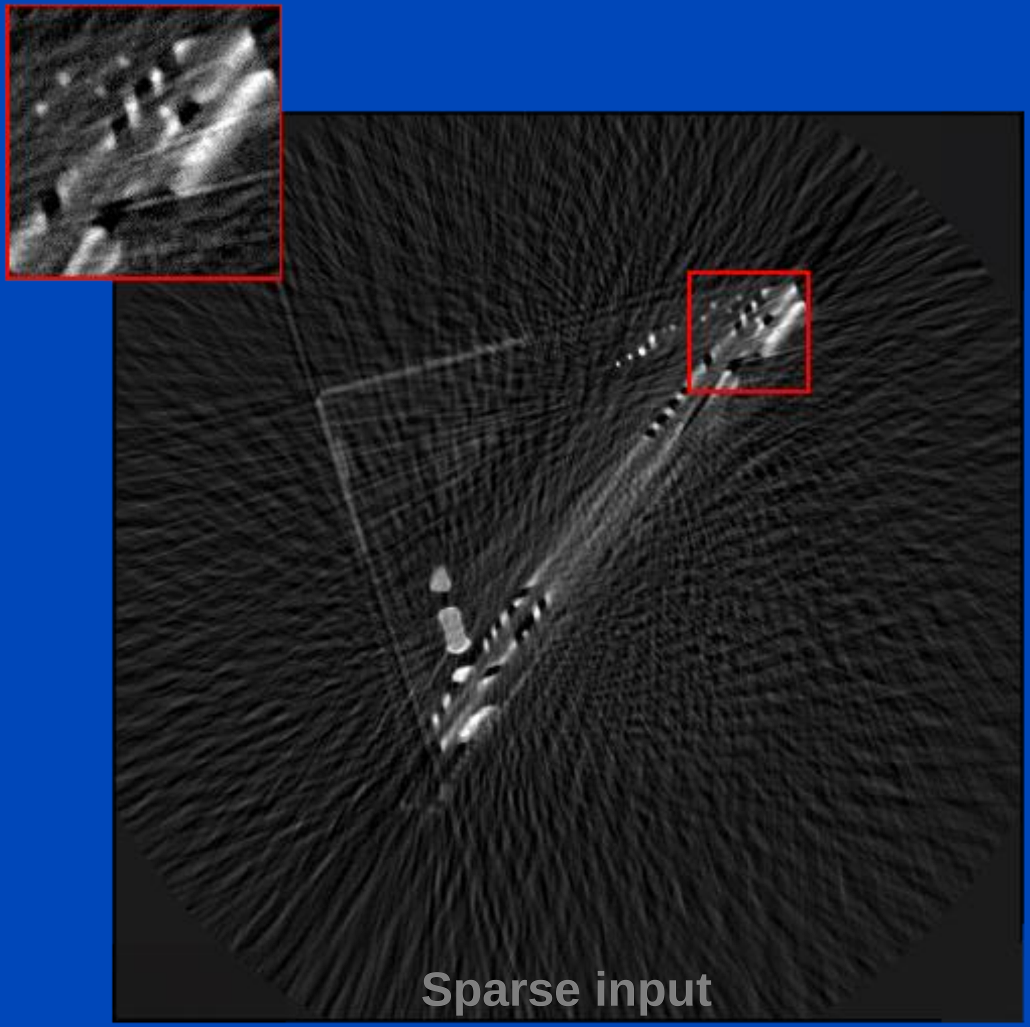

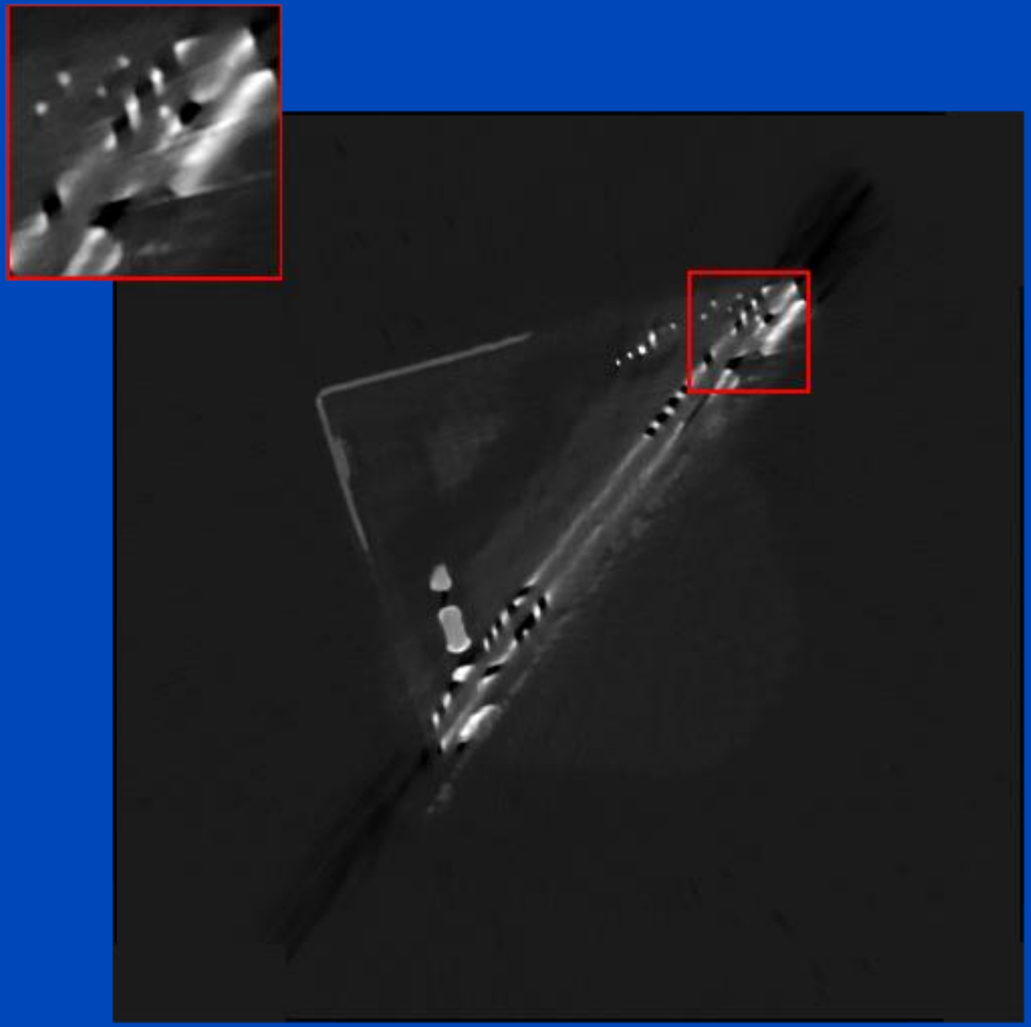

Standard reconstruction

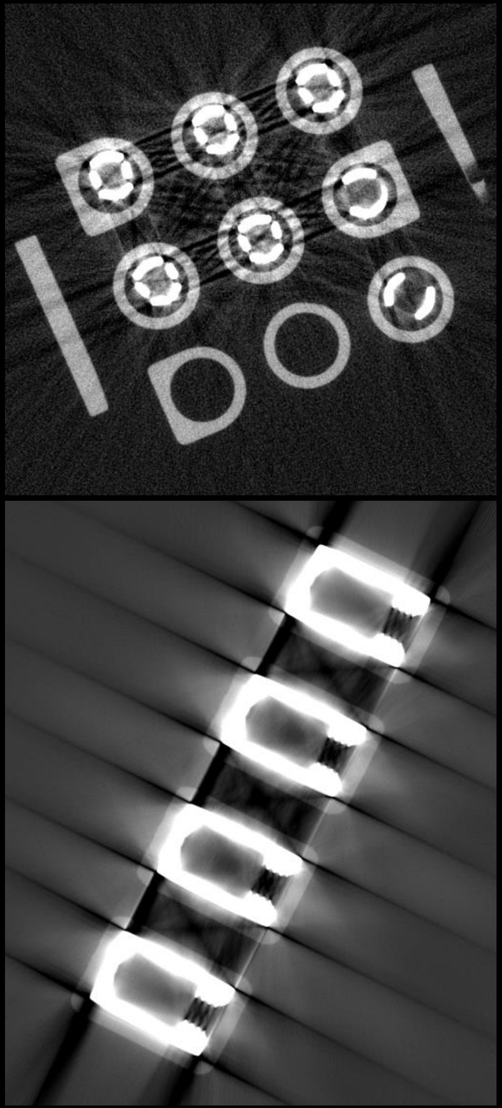

Simulation-based artifact correction

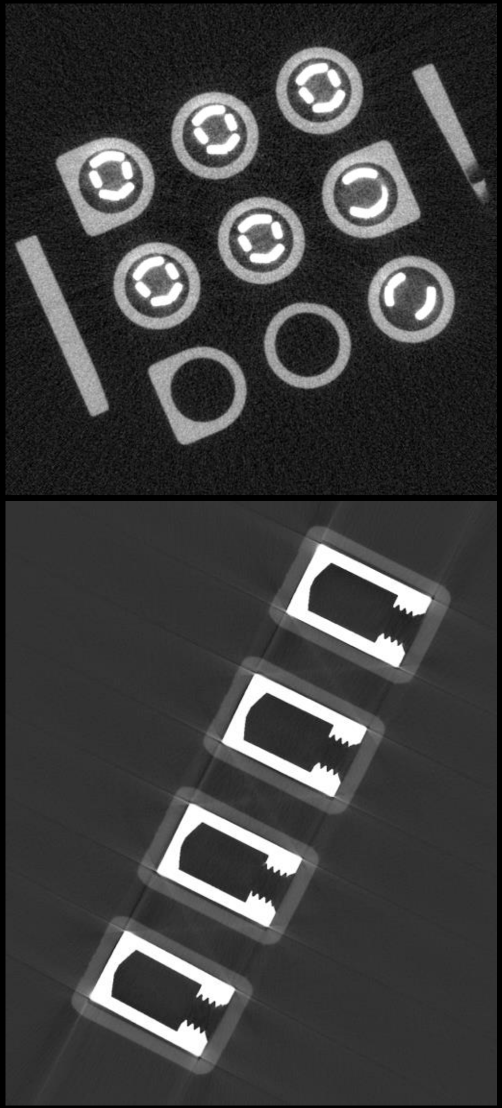

Simulation-based removal of
- beam hardening artifacts
- off-focal radiation artifacts
- focal spot blurring artifacts
- detector blurring artifacts
- **scatter artifacts**
- …

Presented at iCT 2016

J. Maier, M. Kachelrieß et al. Simulation-based artifact correction (SBAC) for metrological computed tomography. Meas. Sci. Technol. 28(6):065011, May 2017.

Deep Scatter Estimation (DSE)

TOP DOWNLOADED PAPER 2018-2019

CONGRATULATIONS TO

Marc Kachelriess

whose paper has been recognized as
one of the most read in

Medi

WILEY

MEDICAL PHYSICS

The International Journal of Medical Physics Research and Practice

Congratulations — your work was one of the top downloaded in recent publication history!

Dear MARC,

We are excited to share that your research, published in *Medical Physics*, is among the top 10% most downloaded papers!

- Real-time scatter estimation for medical CT using the deep scatter estimation: Method and robustness analysis with respect to different anatomies, dose levels, tube voltages, and data truncation

This work received the
Behnken-Berger Award
at the DGMP annual meeting 2021

BEHNKEN-BERGER STIFTUNG

OP DOWNLOADED PAPER 2018-2019

CONGRATULATIONS TO

Joscha Maier

whose paper has been recognized as
one of the most read in

Medical Physics

Monte Carlo Scatter Estimation

- Simulation of photon trajectories according to physical interaction probabilities.
- Simulating a large number of photon t approximates the actual scatter distrib

1 to 10 hours
per tomographic data set

Complete scatter distribution

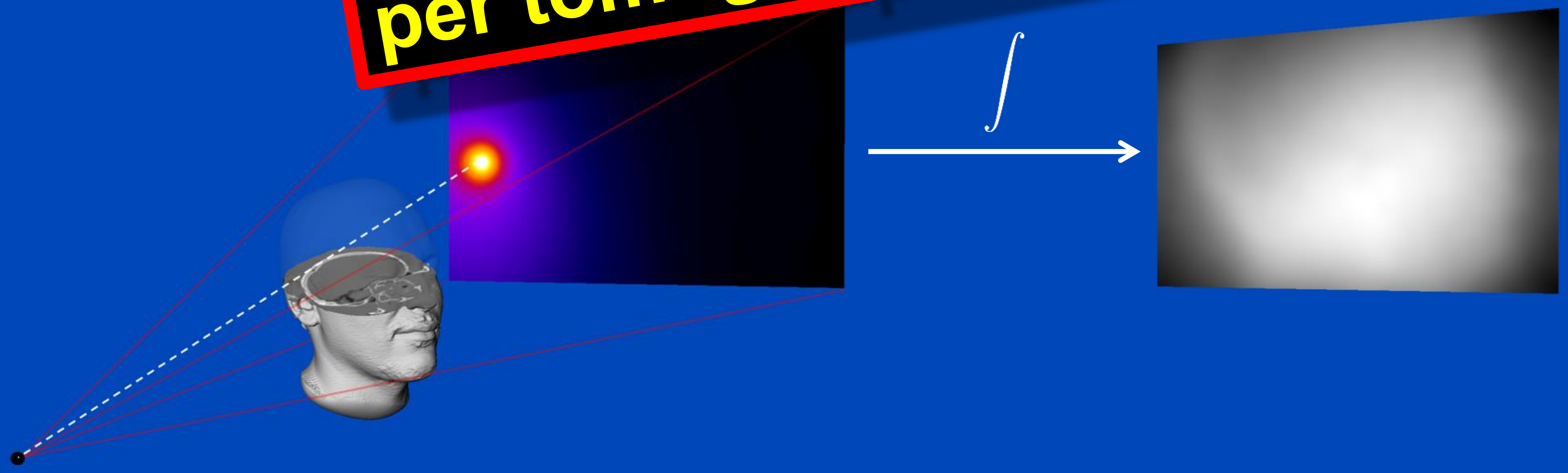

Deep Scatter Estimation

Network architecture & scatter estimation framework

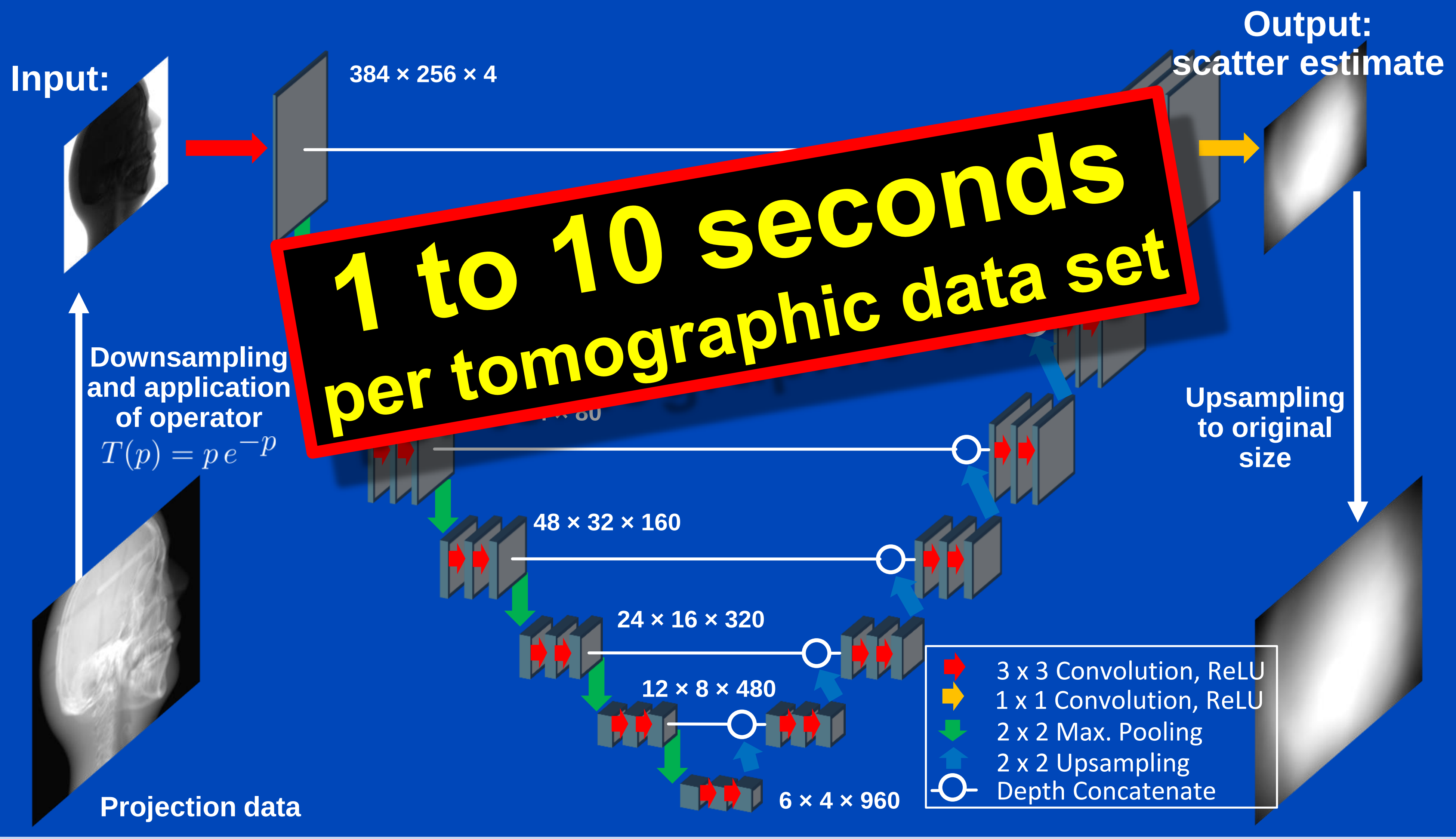

J. Maier, M. Kachelrieß et al. Deep scatter estimation (DSE). SPIE 2017 and Journal of Nondestructive Evaluation 37:57, July 2018.
J. Maier, M. Kachelrieß et al. Robustness of DSE. Med. Phys. 46(1):238-249, January 2019.

Simulation Study: Training Data

- Simulation of 16416 projections using different objects and parameter settings to train the DSE network.
- Training on a GeForce GTX 1080 for 80 epochs using the Keras framework, an Adam optimizer and a mini-batch size of 16.

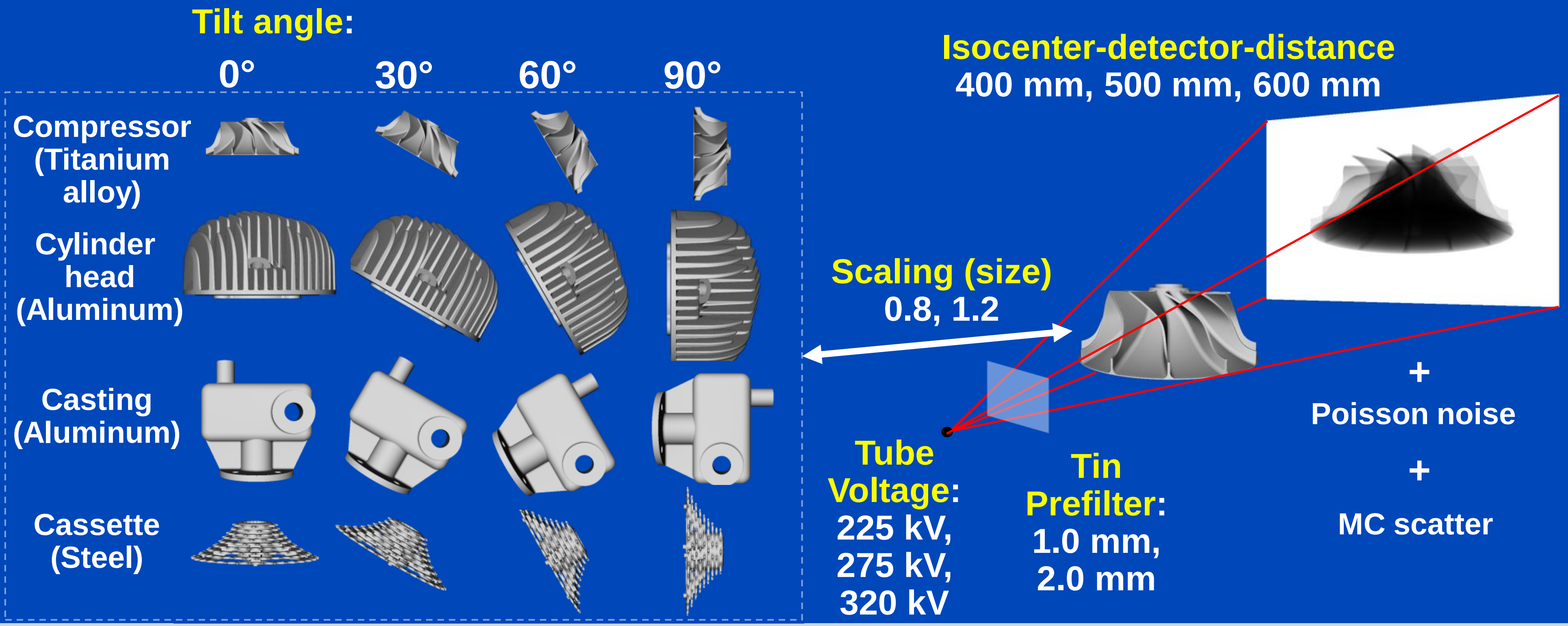

J. Maier, M. Kachelrieß et al. Deep scatter estimation (DSE). SPIE 2017 and Journal of Nondestructive Evaluation 37:57, July 2018.
J. Maier, M. Kachelrieß et al. Robustness of DSE. Med. Phys. 46(1):238-249, January 2019.

Simulation Study: Testing Data

- Simulation of a tomography (720 projection / 360°) of five components using acquisition parameters that differ from the ones used to generate the training data set.

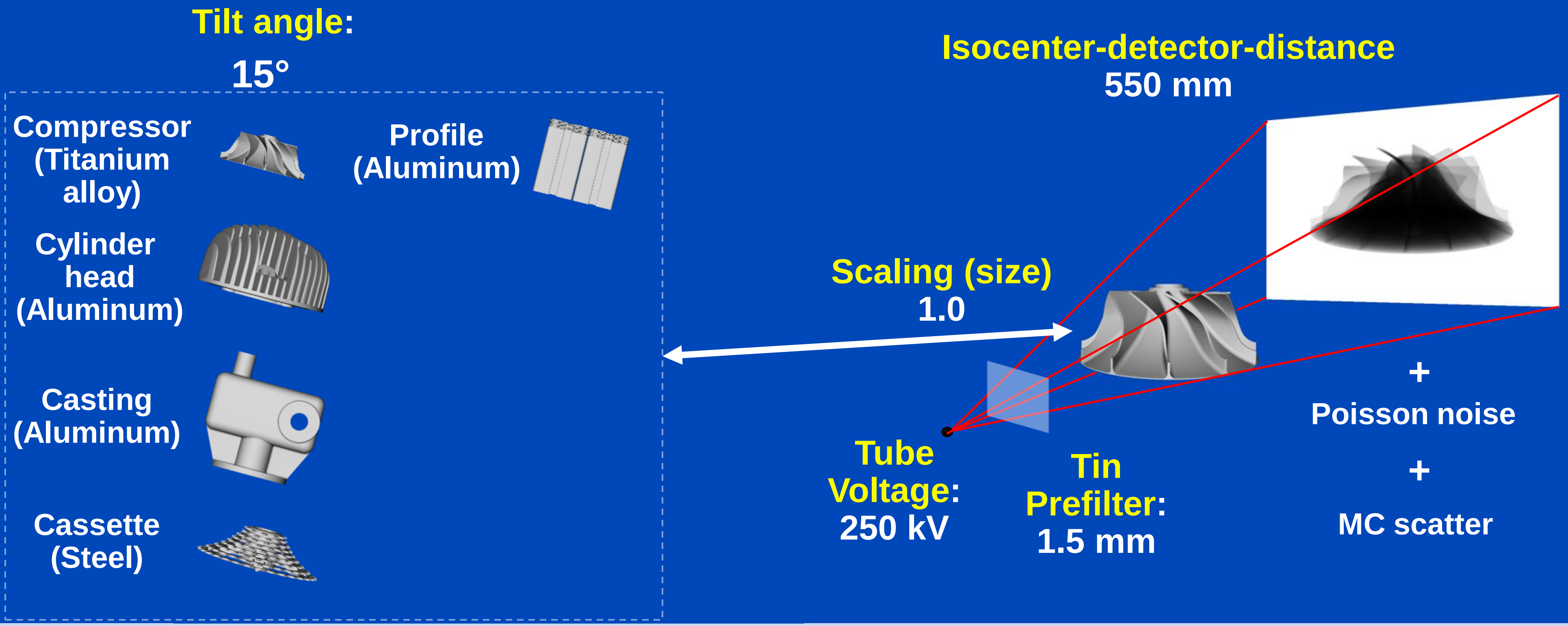

J. Maier, M. Kachelrieß et al. Deep scatter estimation (DSE). SPIE 2017 and Journal of Nondestructive Evaluation 37:57, July 2018.
J. Maier, M. Kachelrieß et al. Robustness of DSE. Med. Phys. 46(1):238-249, January 2019.

Results

Scatter estimates for simulated testing data

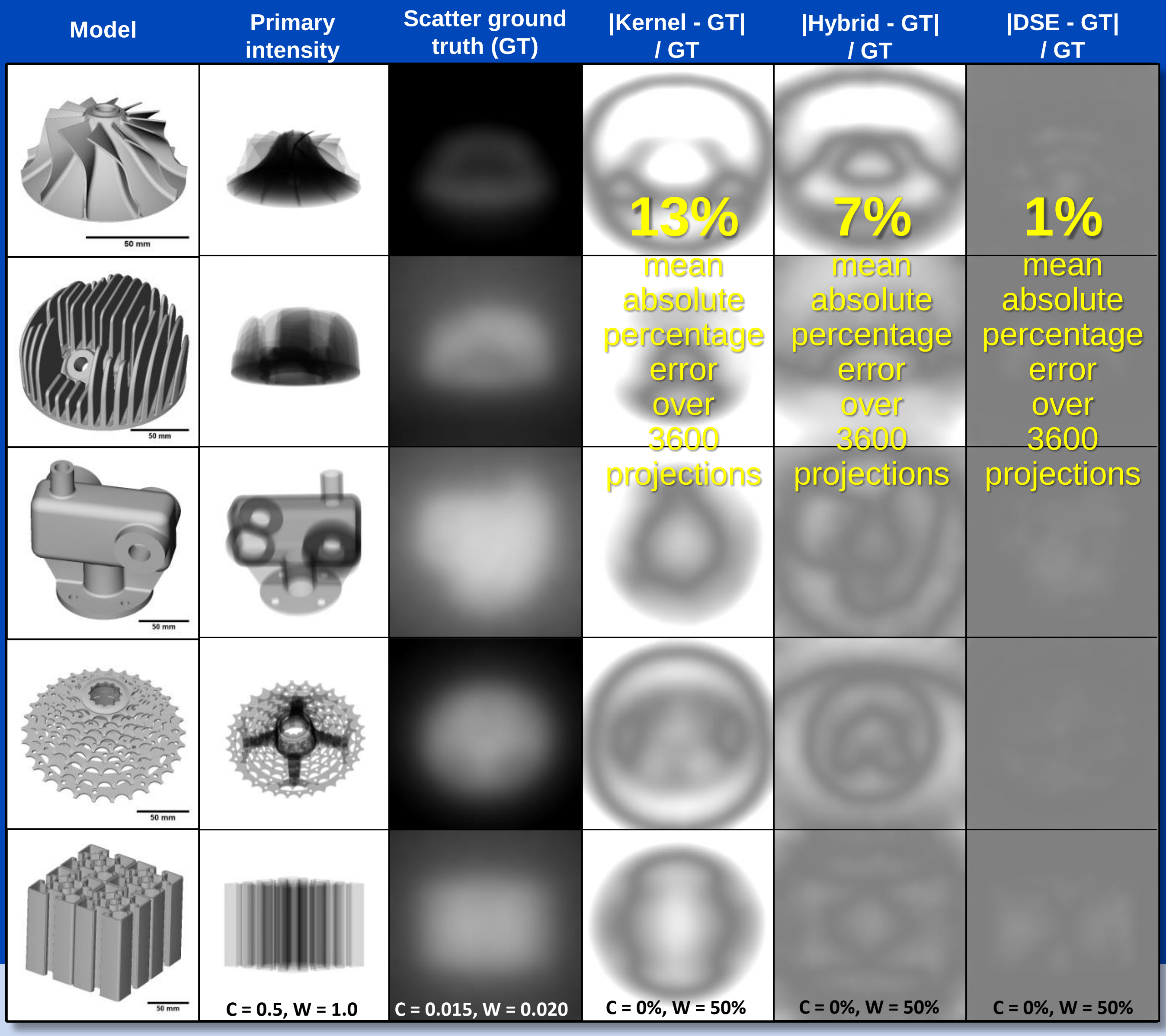

Results

CT reconstructions of scatter corrected testing data

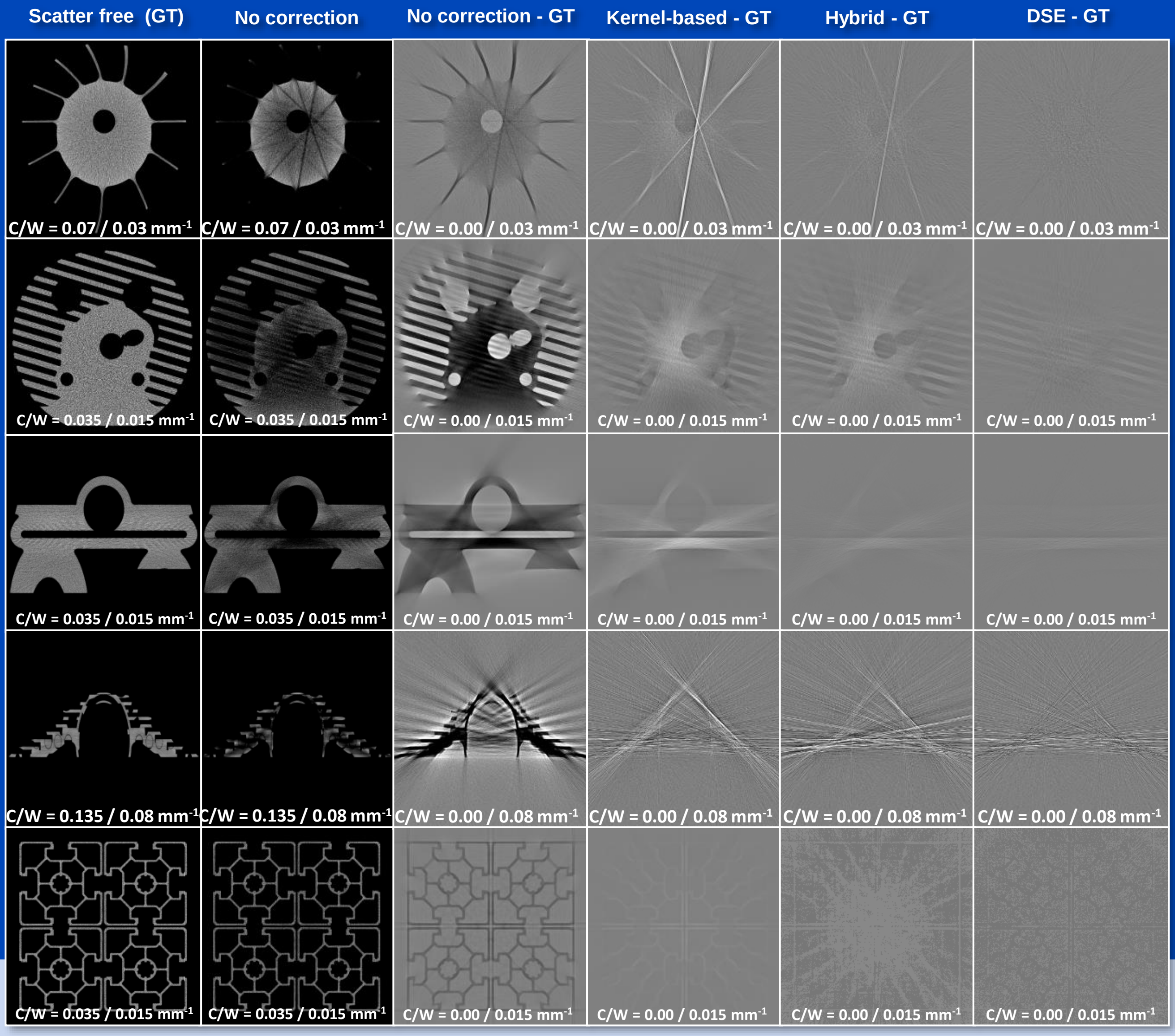

Application to Measured Data

- Measurement at DKFZ table-top CT
- Tomography of aluminum profile
- 720 projections, 360°
- 110 kV Hamamatsu micro-focus tube
- Varian flat detector

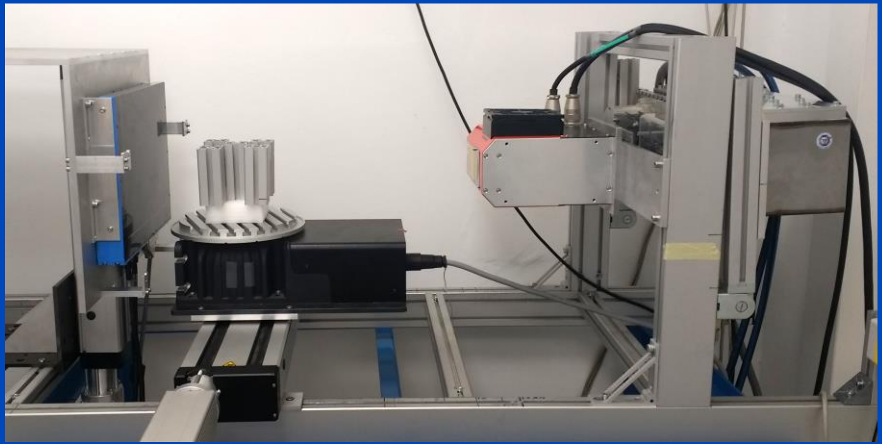

	Training	Testing
Components	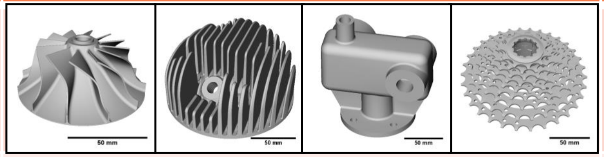	
Detector elements	768×768	768×768
Source-detector distance	580 mm	580 mm
Source-isocenter distance	100 mm, 110 mm, 120 mm	110 mm
Tilt angle	0°, 30°, 60°, 90°	0°
Tube voltage	100 kV, 110 kV, 120 kV	110 kV
Copper prefilter	1.0 mm, 2.0 mm	2.0 mm
Scaling	1.0	-
Number of projections	8208	720

Results

Performance of DSE for measured data

Projection data

Component | MC scatter | |Kernel-based - MC| / MC | |Hybrid - MC| / MC | |DSE - GT| / MC

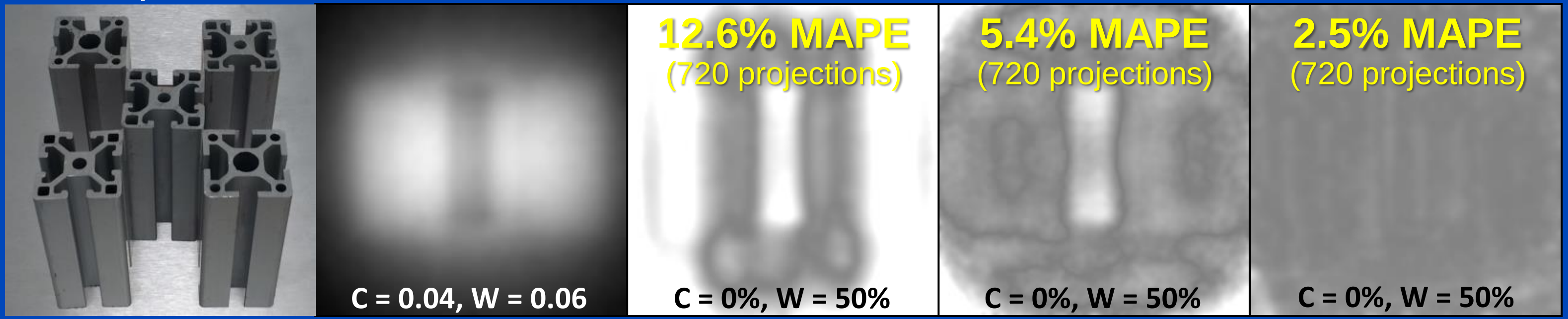

Reconstructions

Monte Carlo (GT) | No correction | Kernel-based | Hybrid | DSE

CT reconstruction

Difference to Monte Carlo

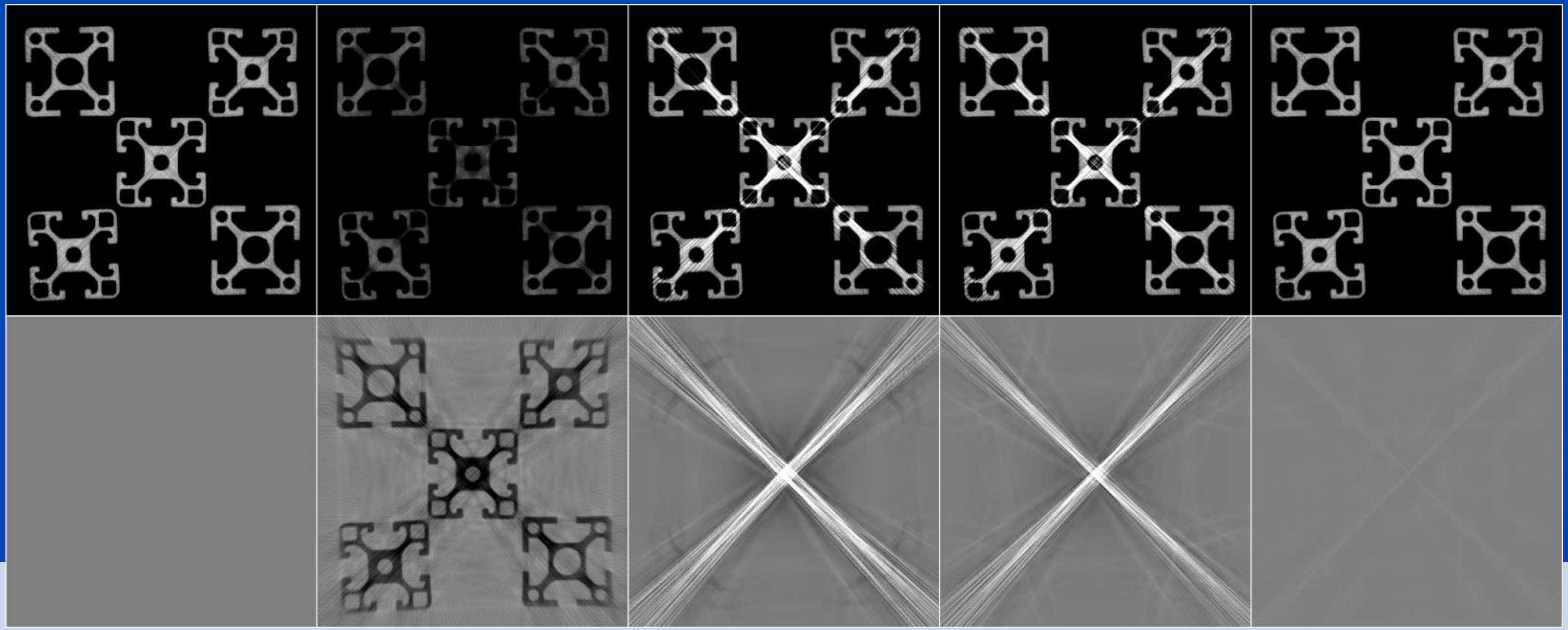

A simple detruncation was applied to the rawdata before reconstruction. Images were clipped to the FOM before display. C = -200 HU, W = 1000 HU.

Truncated DSE

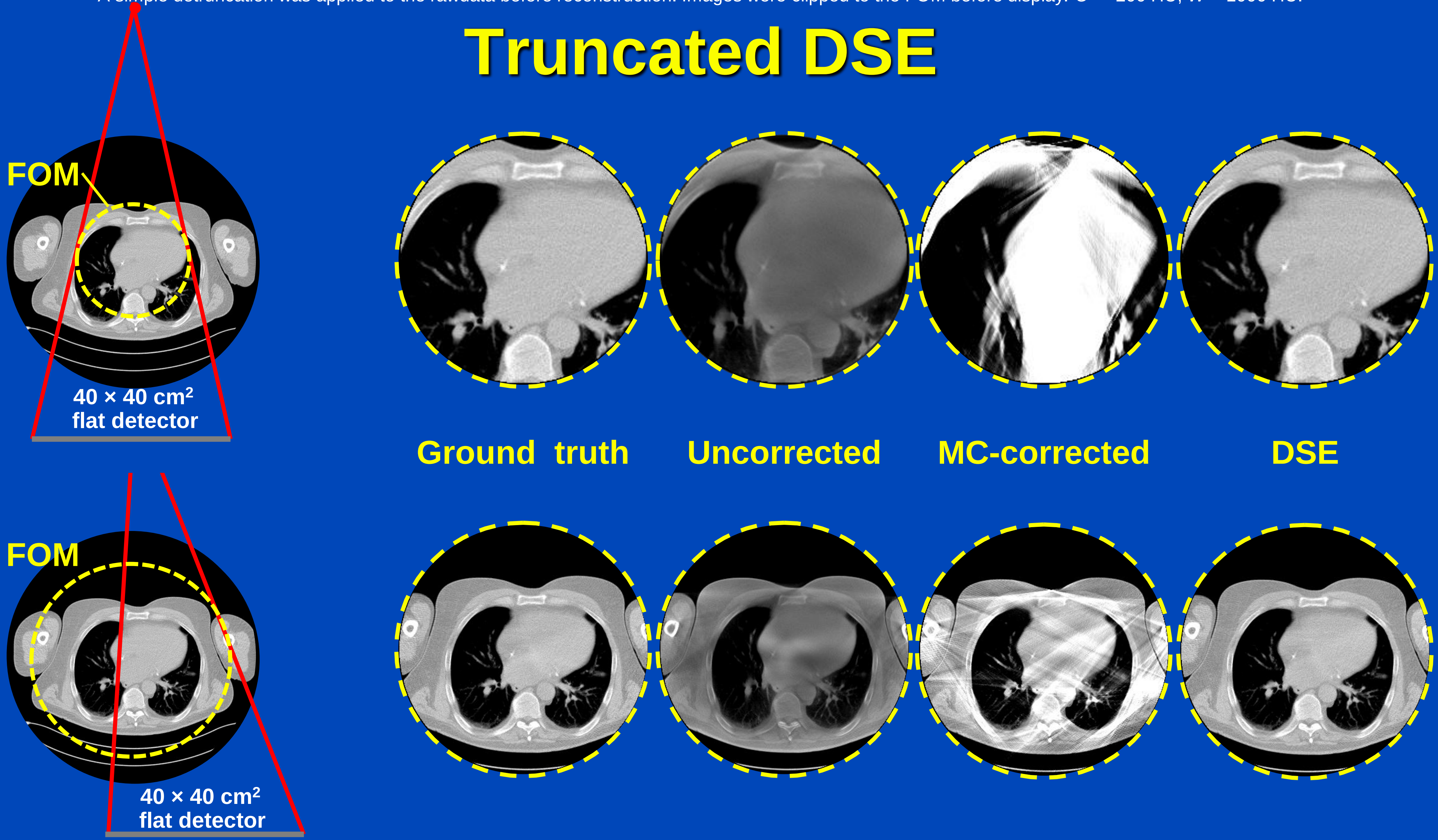

To learn why MC fails at truncated data and what significant efforts are necessary to cope with that situation see [Kachelrieß et al. Effect of detruncation on the accuracy of MC-based scatter estimation in truncated CBCT. Med. Phys. 45(8):3574-3590, August 2018].

J. Maier, M. Kachelrieß et al. Deep scatter estimation (DSE). SPIE 2017 and Journal of Nondestructive Evaluation 37:57, July 2018.
J. Maier, M. Kachelrieß et al. Robustness of DSE. Med. Phys. 46(1):238-249, January 2019.

DSE for Cross-Scatter Correction (xDSE)

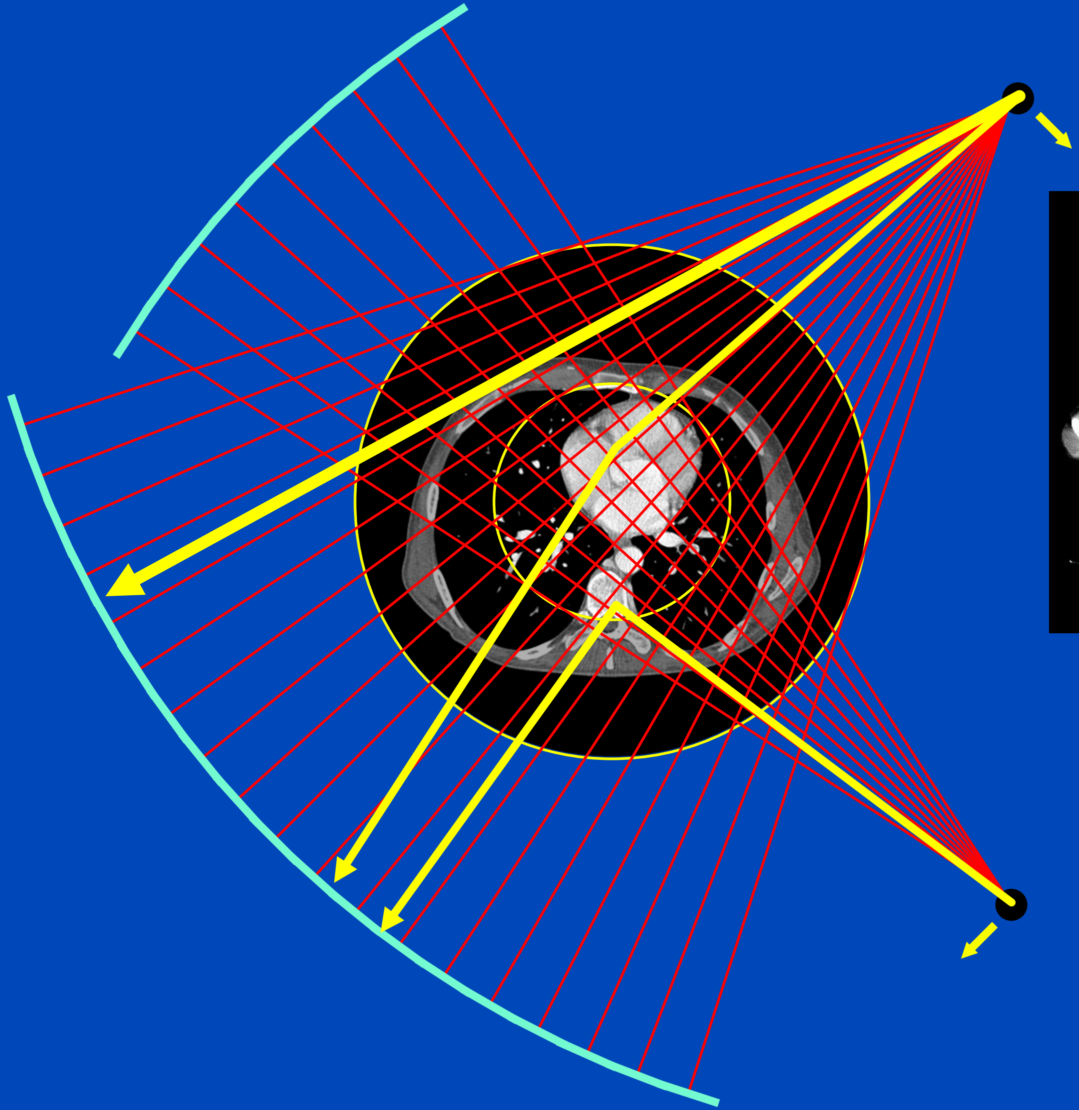

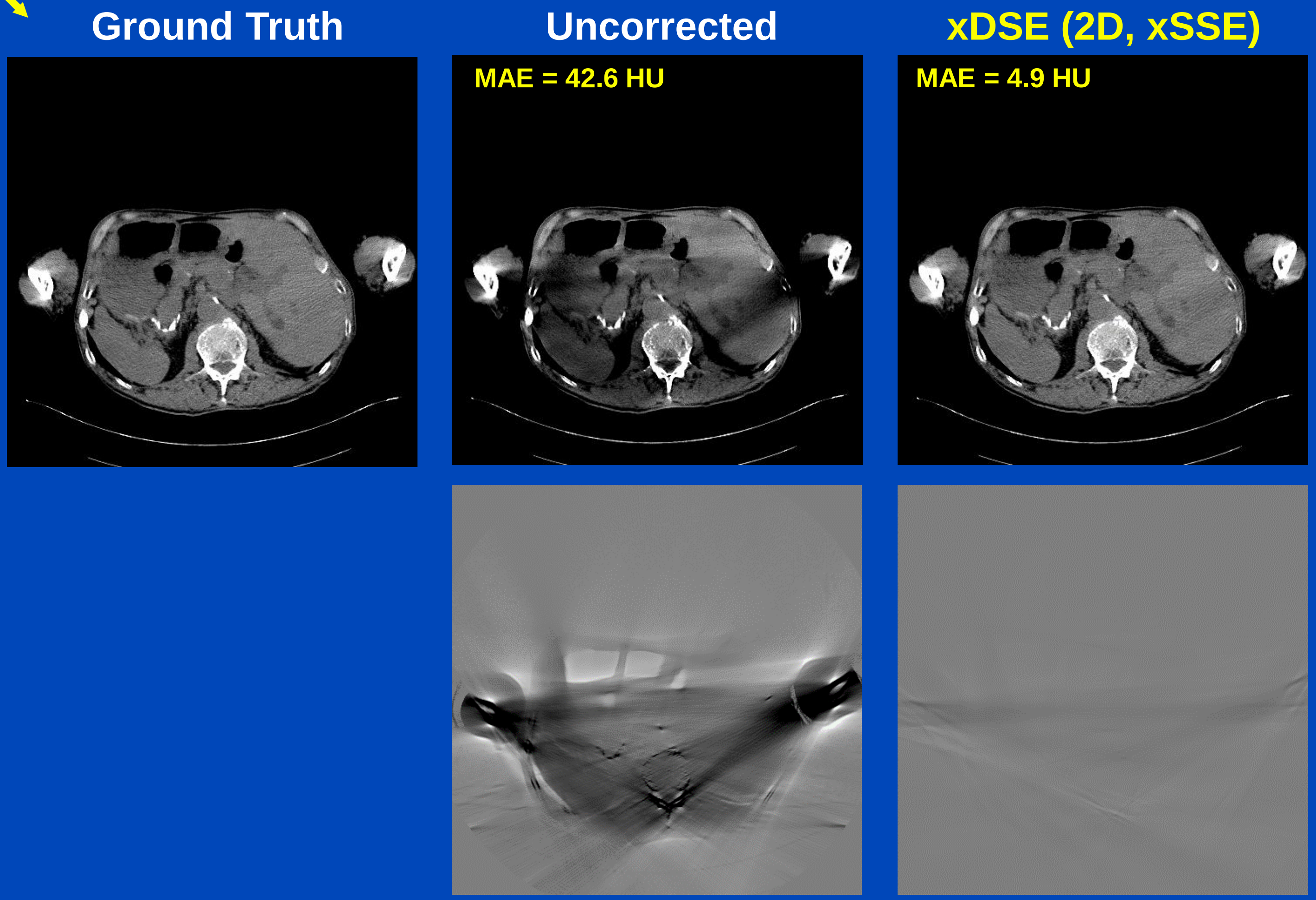

Images C = 40 HU, W = 300 HU, difference images C = 0 HU, W = 300 HU

J. Erath, T. Vöth, J. Maier, E. Fournié, M. Petersilka, K. Stierstorfer, and M. Kachelrieß. Deep learning-based forward and cross-scatter correction in dual source CT. Med. Phys. 48:4824–4842, July 2021.

DSE for Coarse ASG

Coarse ASG
Naeotom Alpha
1376 × 144 macro pixels
pixel size 0.3 × 0.352 mm at iso

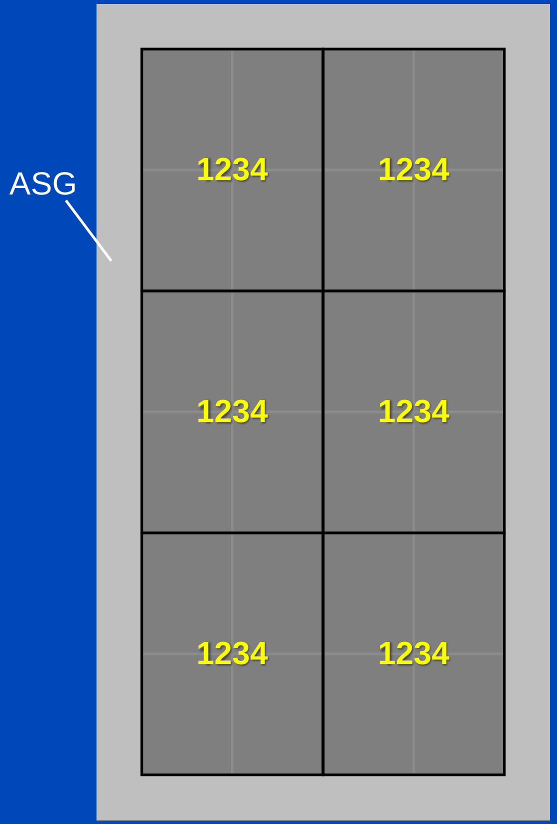

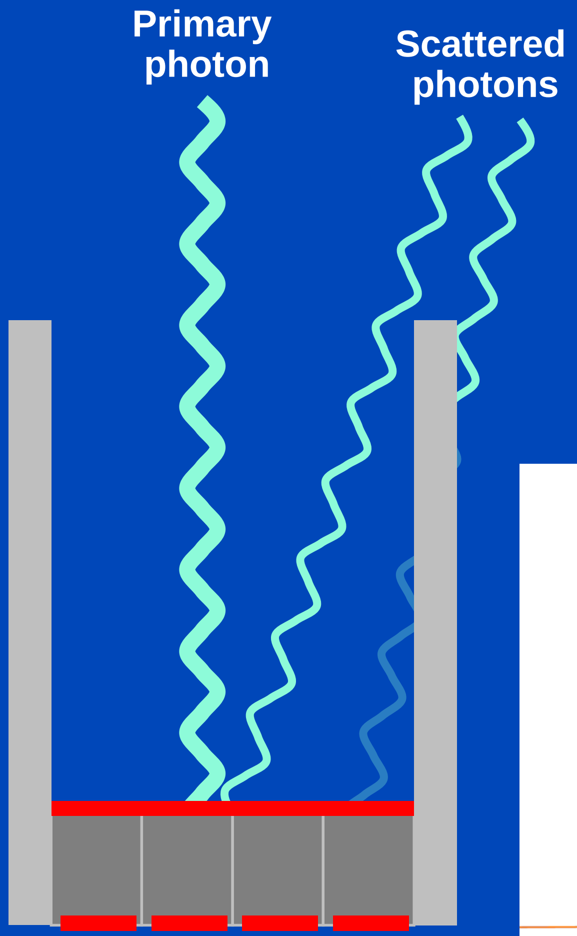

Coarse ASGs lead to changing scatter intensity between neighboring pixels.

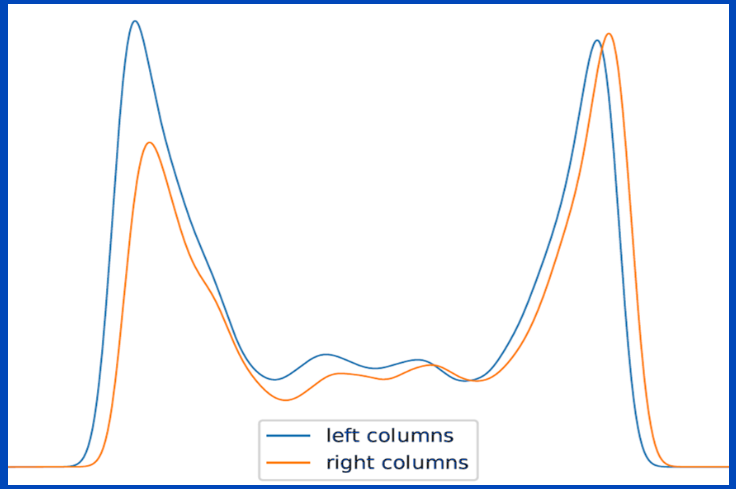

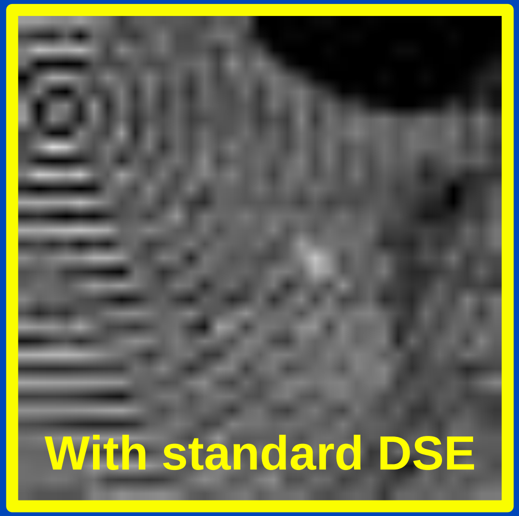

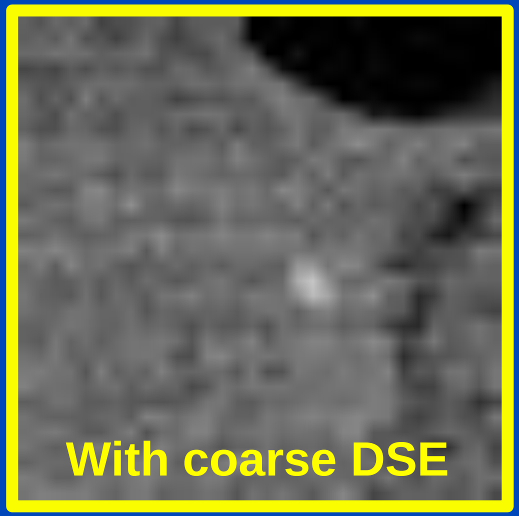

Conclusions on DSE

- DSE needs about 1 ms per projection.
- DSE is a fast and accurate alternative to MC simulations.
- DSE outperforms other approaches in terms of accuracy and speed.
- Facts:
  - DSE can estimate scatter from a single (!) x-ray image.
  - DSE generalizes well to different geometries, scanners and objects.
  - DSE variants for cross-scatter and coarse ASG scatter prediction are available.
  - DSE may outperform MC even though DSE is trained with MC.
- DSE is not restricted to reproducing MC scatter estimates.
- DSE can rather be trained with any other scatter estimate, including those based on measurements.
- DSE can also be used to simulate scatter (at somewhat lower accuracy).

J. Maier, M. Kachelrieß et al. Deep scatter estimation (DSE). SPIE 2017 and Journal of Nondestructive Evaluation 37:57, July 2018.
J. Maier, M. Kachelrieß et al. Robustness of DSE. Med. Phys. 46(1):238-249, January 2019.

uDSE – Basis Principle

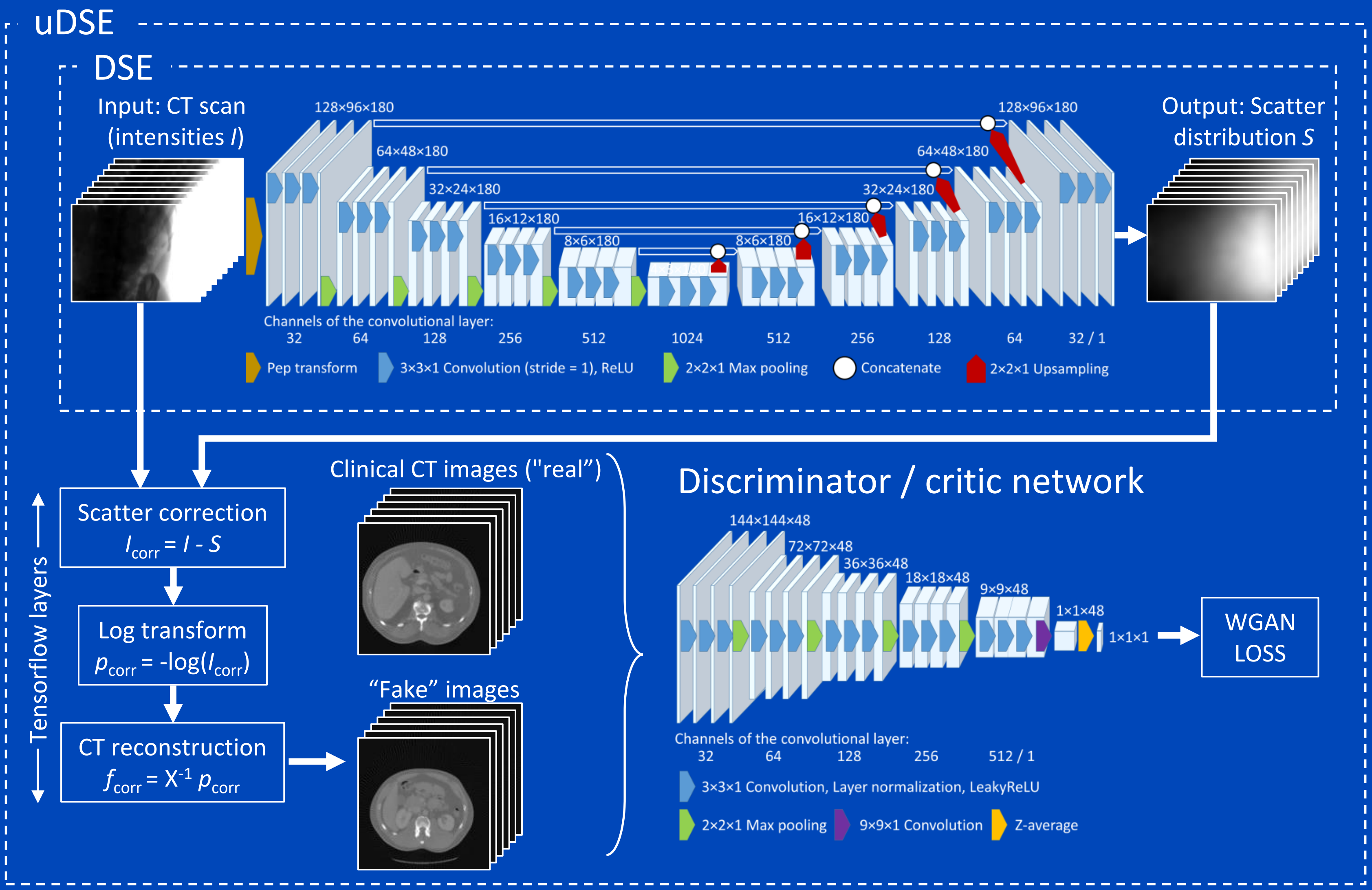

Results

Scatter Estimates

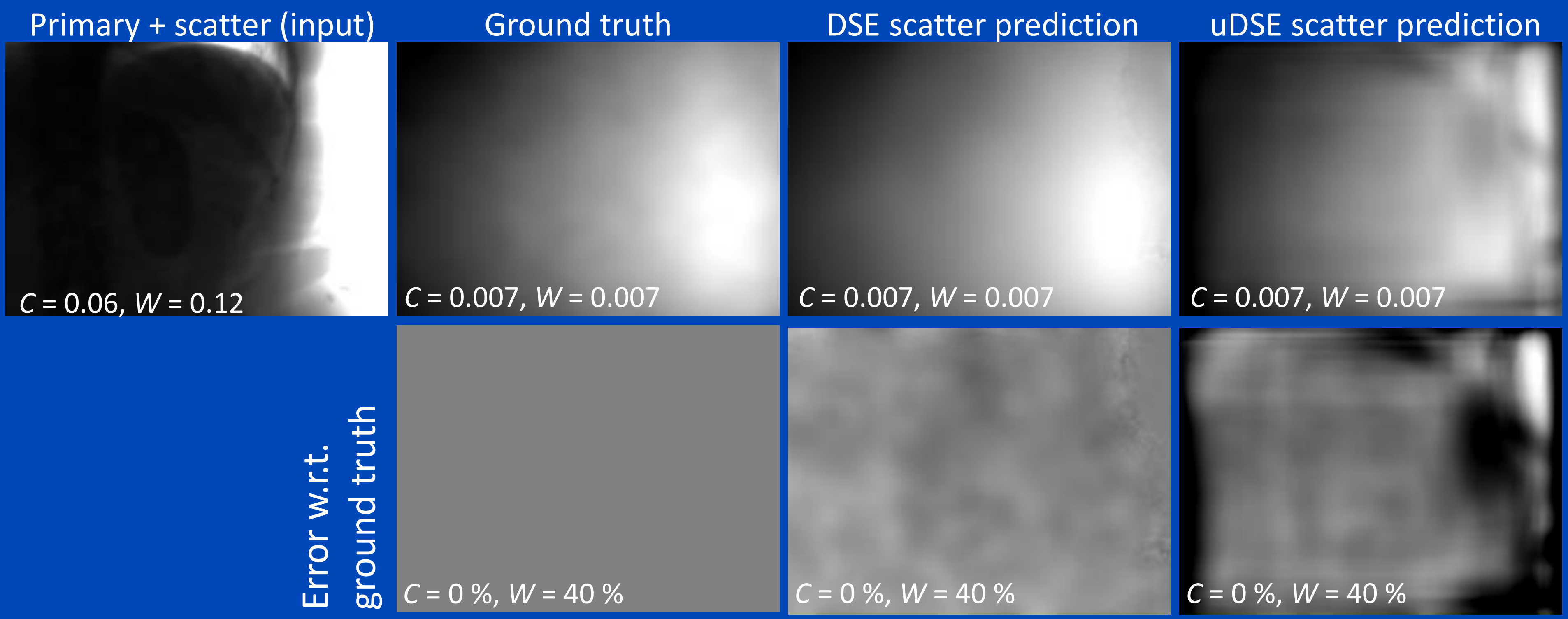

Results

CT Reconstructions

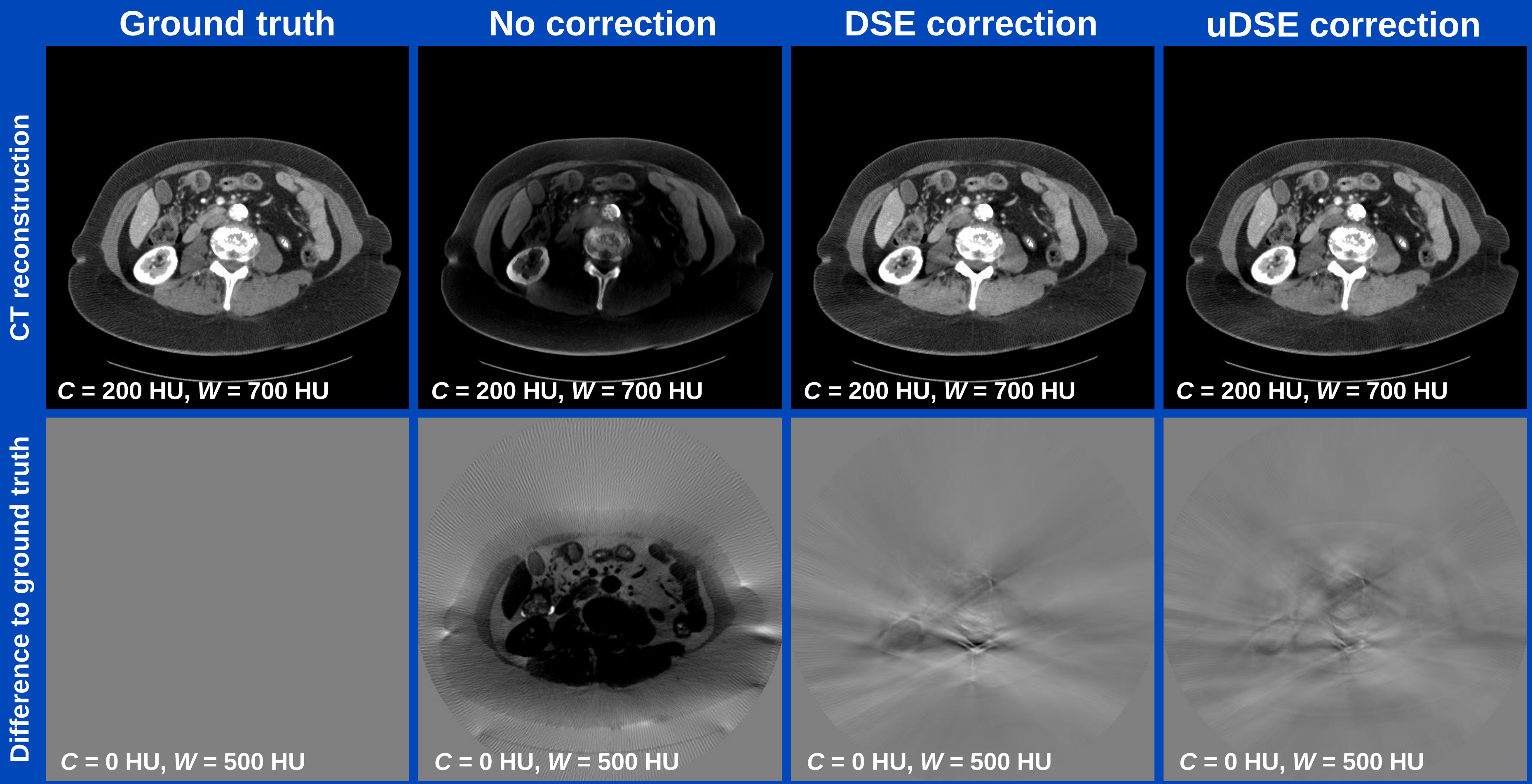

Summary on AI for CT Image Formation

- Powerful tool that allows to solve yet unsolved problems
  - Underdetermined situations, where AI brings in prior knowledge
  - Computational demanding problems, where AI reduces the compute time
  -
- Results have to be taken with care
  - Images often look great, but are they true?
  - Utilizing too much prior knowledge will result in fake content
  - Proves do not exist, the networks‘ output cannot be eplained
  -
- Vendors may tend to overemphasize the benefits from AI
  - Sale by nice looking images

Thank You!

- This presentation will soon be available at www.dkfz.de/ct.
- Job opportunities through DKFZ's international PhD or Postdoctoral Fellowship programs (marc.kachelriess@dkfz.de).
- Parts of the reconstruction software were provided by RayConStruct® GmbH, Nürnberg, Germany.

www.ct-meeting.org